

MARTIN MARIETTA ENERGY SYSTEMS LIBRARIES  
3 4456 0361539 0

CENTRAL RESEARCH LIBRARY  
DOCUMENT COLLECTION

ORNL-2991  
Progress

243

OAK RIDGE NATIONAL LABORATORY  
STATUS AND PROGRESS REPORT  
JULY 1960

**CENTRAL RESEARCH LIBRARY  
DOCUMENT COLLECTION  
LIBRARY LOAN COPY  
DO NOT TRANSFER TO ANOTHER PERSON**

If you wish someone else to see this document, send in name with document and the library will arrange a loan.



**OAK RIDGE NATIONAL LABORATORY**  
operated by  
**UNION CARBIDE CORPORATION**  
for the  
**U.S. ATOMIC ENERGY COMMISSION**



Downgrade to Unclassified After August 4, 1961





ORNL-2991

Copy No. \_\_\_\_\_

Contract No. W-7405-eng-26

OAK RIDGE NATIONAL LABORATORY  
STATUS AND PROGRESS REPORT  
JULY 1960

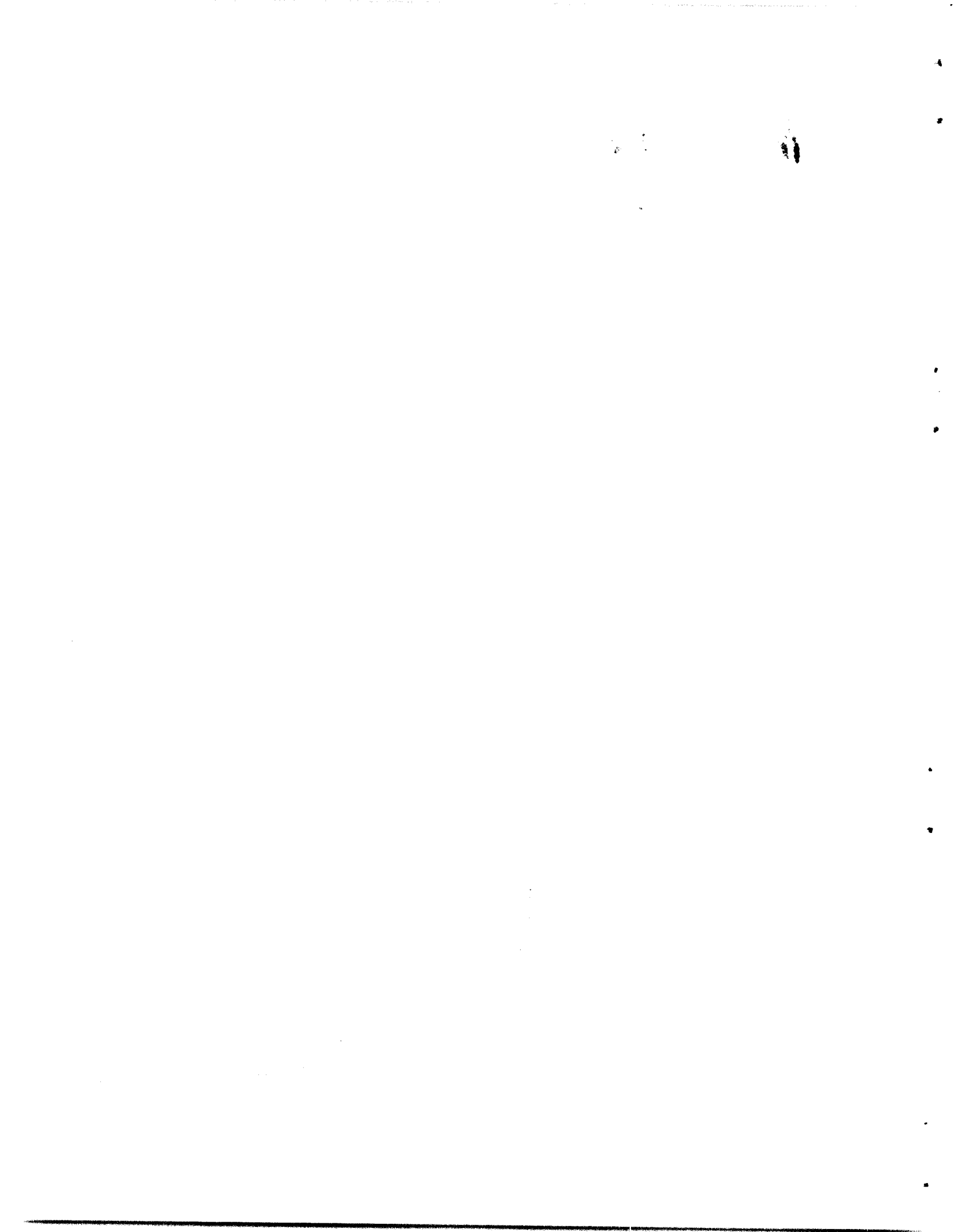
DATE ISSUED

AUG - 4 1960

OAK RIDGE NATIONAL LABORATORY  
Oak Ridge, Tennessee  
operated by  
UNION CARBIDE CORPORATION  
for the  
U.S. ATOMIC ENERGY COMMISSION



3 4456 0361539 0



CONTENTS

SPECIAL NUCLEAR MATERIALS PROGRAM.....	1
Power Reactor Fuel Processing Pilot Plant.....	1
REACTOR DEVELOPMENT PROGRAM.....	1
GAS-COOLED REACTOR PROJECT.....	1
Fission-Gas Release from UO <sub>2</sub> .....	1
Capsule Irradiation Experiments in the ORR.....	2
Closed-Cycle Experiment in the ORR.....	2
GCR-ORR Loop No. 1.....	2
Irradiation Experiments in the MTR.....	2
Reactions of Type 304 Stainless Steel with CO <sub>2</sub> -CO	
Mixtures.....	3
Pressure Vessel Model Tests.....	3
Experimental Model Tests of Fuel Capsule Tubing.....	3
THERMAL-BREEDER REACTOR PROGRAM.....	3
Homogeneous Reactor Program.....	3
Homogeneous Reactor Test.....	3
HRT Chemical Pilot Plant.....	4
Thorium Blanket Studies.....	4
Reactor Analysis.....	4
Homogeneous Reactor Instrumentation.....	5
Metallurgy and Ceramics.....	5
Out-of-Pile Solution Corrosion Tests.....	6
In-Pile Solution Corrosion Tests.....	6
Supporting Radiation Corrosion Studies.....	7
In-Pile Blanket Materials Tests.....	8
MOLTEN-SALT REACTOR PROJECT.....	8
Component Development.....	8
Remote Maintenance.....	9
Chemistry.....	9
Metallurgy.....	9
Corrosion Tests.....	10
Reactor Analysis.....	11
Thorium-Breeder-Reactor Evaluation Studies.....	11
MSRE Design.....	11
HIGH FLUX ISOTOPE REACTOR.....	12
Reactor Physics Calculations.....	12
Heat Transfer.....	12
Critical Experiments.....	13
Corrosion.....	13
Metallurgy: Evaluation of the Mark II-A Test Element.....	14
Metallurgy: Fabrication of the Mark II-B Fuel Element.....	14
Design: Fuel Plate Stability.....	15
Design: Beryllium Reflector.....	15
Design: Shielding of the Reactor Water System.....	15
MARITIME REACTORS PROGRAM.....	16
NUCLEAR TECHNOLOGY AND GENERAL SUPPORT.....	16
Reactor Evaluation Studies.....	16

Radiation Detector Development.....	16
Zirconium Metallurgy.....	16
Fuel Element Development.....	17
Nondestructive Test Development.....	17
Mechanical Properties Research.....	18
Materials Compatibility Studies.....	18
Fuel Cycle Technology.....	19
Power Reactor Fuel Processing: Darex-Thorex Process.....	19
Power Reactor Fuel Processing: Mechanical Processing.....	20
Power Reactor Fuel Processing: Criticality Control.....	20
Power Reactor Fuel Processing: Solvent Extraction.....	20
Power Reactor Fuel Processing: Processes for Graphite- Containing Fuels.....	21
Power Reactor Fuel Processing: Processes for U-Mo Fuels..	21
Power Reactor Fuel Processing: Processes for Zirconium-Containing Fuels.....	22
Power Reactor Fuel Processing: Sulfex Process.....	22
Fluoride Volatility Processing.....	22
PHYSICAL RESEARCH PROGRAM.....	23
Reactor Operations.....	23
Waste Disposal.....	23
PHYSICS AND MATHEMATICS RESEARCH.....	23
Charge Spectrometry.....	23
Neutron Diffraction.....	24
Theoretical Physics.....	24
High-Voltage Experimental Program.....	24
Spectroscopy Research Laboratory.....	24
CHEMISTRY RESEARCH.....	25
Spectrophotometric Studies of Solutions at Elevated Temperatures and Pressures.....	25
Raw Materials Research and Development.....	25
Solvent Extraction Research.....	25
Ion Exchange Technology.....	26
Mechanisms of Separations Processes.....	26
High-Temperature Aqueous Solution Chemistry.....	27
Reactor Neutron Cross Sections.....	27
Nuclear Chemistry: Characterization of Short-Lived Fission Products.....	28
Electrochemical Kinetics and Its Application to Corrosion.....	28
Chemical Separation of Isotopes.....	29
Chemical Applications of Nuclear Explosions.....	29
METALLURGY AND MATERIALS RESEARCH.....	30
Ceramics Research.....	30
CONTROLLED THERMONUCLEAR RESEARCH.....	30
Cross-Section Studies.....	30
DCX-1 Facility.....	30
DCX-EPA.....	31
Ion Source Development.....	31

Theory.....	31
BIOLOGY AND MEDICINE PROGRAM.....	31
RADIATION EFFECTS ON BIOLOGICAL SYSTEMS.....	31
Cell Growth and Reproduction.....	31
Pathology and Physiology.....	32
Biophysics: Magnetic Resonances.....	32
Biophysics: Ultraviolet Studies.....	32
Chemical Protection and Enzyme Catalysis.....	33
COMBATING RADIATION DETRIMENTAL EFFECTS.....	33
Radiation Protection: Living Cells.....	33
Mammalian Radiation Recovery.....	33
Radiation Immunology.....	33
BIOMEDICAL PROBLEMS IN ATOMIC ENERGY OPERATIONS.....	34
Basic Instrumentation.....	34
OPEN LITERATURE PUBLICATIONS.....	35
VISITORS.....	38



OAK RIDGE NATIONAL LABORATORY

STATUS AND PROGRESS REPORT

July 1960

This Status and Progress Report summarizes that portion of the Laboratory's work which is unclassified. Some of the topics are included every month, but the majority are reported on a bimonthly schedule.

SPECIAL NUCLEAR MATERIALS PROGRAM

Power Reactor Fuel Processing Pilot Plant. - Cleanup of contamination resulting from an explosion of an evaporator loop in Building 3019 was continued. All areas of the building except the process cells and one basement area have been cleaned and painted. Air contamination in all areas outside the cells has been below the maximum permissible concentration for plutonium for the past two months. Building modifications for improved interim containment of cells 3, 4, 5, 6, and 7 are essentially complete. Installation of the vessel off-gas header to the 3039 stack is complete except for final connections at the stack and at Building 3019.

REACTOR DEVELOPMENT PROGRAM

GAS-COOLED REACTOR PROJECT

Fission-Gas Release from UO<sub>2</sub>. - Changes in the fission-gas retention characteristics of the thin plates of UO<sub>2</sub> being studied in the ORR instantaneous-fission-gas-release experiment indicated, as discussed previously (ORNL-2980), that the oxygen-to-uranium ratio in the UO<sub>2</sub> had increased to at least 2.08. Therefore an effort was made to reduce the oxygen-to-uranium ratio by adding hydrogen to the sweep gas. In these experiments, steady-state fission-gas release conditions were established with pure helium as the atmosphere before the hydrogen-bearing sweep gas was introduced. The hydrogen-bearing gas caused an immediate increase in the fission-gas release rate that peaked at about three times the steady-state release rate, and then slowly decreased until, within 16 hr, the release rate was less than one-half the previous steady-state release rate. The hydrogen-bearing sweep gas is still being used, and the fission-gas release rate is continuing to decrease slowly. The fission-gas release burst observed when the hydrogen reached the fuel was the first burst observed in these experiments that did not involve a temperature change. Further, the burst did not involve a

[REDACTED]

change in the composition of the released fission gas, only a change in magnitude.

A postirradiation measurement was made of the gas pressure in capsule O-6, a full-diameter prototype EGCR fuel capsule consisting of  $UO_2$  pellets in a stainless steel capsule that had been irradiated in the ORR at a cladding temperature of  $1600^\circ F$  to a burnup of 1980 Mwd/metric ton. The gas pressure was measured while the capsule was being heated to  $1725^\circ F$  in order to study the contribution of cesium and iodine compounds. A plot of the gas pressure vs temperature gave the straight line predicted by the gas laws for krypton and xenon release and therefore indicated no volatilization of cesium and iodine compounds.

Capsule Irradiation Experiments in the ORR. - Irradiation of the eight group II capsules was satisfactorily completed when the ORR ended cycle XXV. All capsules were withdrawn from the reactor poolside facility and, later, placed in temporary storage to await disassembly. During the period of irradiation of these capsules, seven reactor cycles (XIX through XXV), the accumulated reactor power generation was  $\sim 67,000$  Mwhr or 139 equivalent full power (20 Mw) days. The estimated burnups for the capsules are in the range 1250 to 2320 Mwd/metric ton.

The capsule mounting plates were replaced with those to be used for the group III capsules, and the shutters were removed. New, individual "chimney"-type shutters have been designed and constructed for installation along with the group III capsules.

Two beryllium-clad capsules were received from the UKAEA on June 22, and five French capsules were received on July 1. Two of the French capsules, O3 and O8, were selected for irradiation. One ORNL capsule, ORNL-1B-2, a counterpart of the British capsules, was completed on July 7. The two British, two French, and one ORNL capsule are being prepared for irradiation.

Closed-Cycle Experiment in the ORR. - Sampling of the sweep gas with the second fuel capsule in both the inserted and withdrawn positions has shown clearly that the activity in the gas is from material deposited in the in-pile tubes when the first fuel capsule failed; the activity has not increased to above that present before the second capsule was irradiated. The capsules being studied in these experiments consist of  $UO_2$  encased in siliconized silicon carbide-coated graphite.

GCR-ORR Loop No. 1. - Leak testing and instrumentation and controls checkout at the ORR continued satisfactorily. Installation of the in-pile section thermocouple leads and seal was completed. A flux-monitoring tube and flange-alignment dowel holes are being added. The mockup fuel element assembly was tested successfully in the in-pile section.

Irradiation Experiments in the MTR. - The second  $UC_2$ -graphite experimental assembly, ORNL-MTR-48-2, was installed in the MTR and is operating normally, with very little fission gas in evidence in the helium purge gas that bathes the graphite capsule surface. An increase in purge gas activity from about 6 to  $30$  mc/cm<sup>3</sup> occurred over a 24-hr period (July 6 and 7); the cause of the increased activity is unknown.

Reactions of Type 304 Stainless Steel with CO<sub>2</sub>-CO Mixtures. - Compatibility tests are in progress of type 304 stainless steel specimens in a CO-CO<sub>2</sub> gas mixture with a CO<sub>2</sub>-to-CO ratio of 0.4 and a total CO + CO<sub>2</sub> content of approximately 0.5 vol % in helium carrier gas. In these tests, which are designed for studying the effects of time and temperature on oxidation, carburization, and soot deposition, the metal temperatures range from 500 to 1800°F. Approximately 700 hr of the planned 1000-hr test period has elapsed.

Pressure Vessel Model Tests. - All strain gages were installed and wiring was completed on the 1/6-scale model of the EGCR pressure vessel head. Strain measurements were made for the following loading conditions:

1. internal pressure of 60 psig,
2. axial load on an outer control rod nozzle of 2000 lb,
3. axial load on an inner special nozzle of 1500 lb,
4. axial load on an outer special nozzle of 1500 lb,
5. axial load on a large in-pile loop nozzle of 2000 lb,
6. axial load on the central control rod nozzle of 2000 lb,
7. axial load on a small in-pile loop nozzle of 1500 lb,
8. combined loading with internal pressure of 60 psig and axial load of 2000 lb on the central control rod nozzle.

The total stresses, the membrane stresses, and the bending stresses were then calculated for each gage position on the spherical dome and cylinder, and the results are being checked and analyzed.

Experimental Model Tests of Fuel Capsule Tubing. - Four 12-in.-long tubular specimens of type 304 stainless steel (0.750-in. OD, 0.025-in. wall) are being tested at 1200°F with an external pressure of 400 psi. The test was interrupted at 508 and at 1252 hr for specimen examination. No evidence of collapse was found, and the test is being continued.

Four other specimens identical to those described above are being tested at 1200°F with an external pressure of 600 psi. After 475 hr of the test, failure of the furnace and a bulge on the pressure container necessitated examination of the test system. Measurements of the specimens showed no collapse.

One specimen of the same configuration was heated to 1200°F, and the external pressure was increased until collapse occurred. The collapse was instantaneous, and it occurred at an external pressure of 800 psi.

## THERMAL-BREEDER REACTOR PROGRAM

### Homogeneous Reactor Program

Homogeneous Reactor Test. - Work on modifying and repairing the HRT core vessel continued. The upper (second) core-vessel hole was enlarged with a remote cutting tool which removed samples of the Zircaloy tank. Preliminary metallographic examination of the metal indicates that the edge of the hole had once been molten. The sample itself was ductile. Following sampling of the core wall, the hole was reamed to provide a seating surface for the Zircaloy plug which is to seal the hole.

Another impression of the lower hole was taken by using a precut plastic block which had the approximate shape of the hole. A Zircaloy patch was then fabricated from this model.

Both patches will be installed in August.

HRT Chemical Pilot Plant. - Apparent induced-underflow ratios and efficiencies were measured for the new HRT multiclone and for a Dorr-Oliver TM stage modified to give 32 hydroclones in parallel on one induced-underflow receiver. The apparent induced-underflow ratios for the two multiclone units were 2.5 to 5.0 times the experimental and calculated values for single hydroclones of the same dimensions. The efficiencies for  $\text{ThO}_2$  of about 1.6  $\mu$  diameter, corrected for the underflow volume, were 80 to 90% for single hydroclones with continuous underflow, 50 to 60% for the multiclone with 5% of the feed flow as continuous underflow, and 16 to 22% for induced-underflow operation of the multiclone. These results are believed to be due to unequal flows through the underflow ports of the parallel units.

A study was begun to determine the feasibility of purifying the uranium in used HRT fuel from extraneous material by precipitation of uranium peroxide. The effect of mixing rate, temperature, solution pH, and settling time was investigated briefly in laboratory equipment scaled down from the proposed HRT chemical plant equipment. To date, several 30-g batches of uranium have been processed from simulated HRT fuel-solution concentrate with a 95% recovery of uranium and decontamination factors of 100 from copper and 170 from nickel.

Thorium Blanket Studies. - Results of flame denitration runs intended to produce 5- to 10- $\mu$ -dia product instead of 1 to 2  $\mu$  showed no significant product size changes with substitution of  $\text{Th}(\text{SO}_4)_2$  for  $\text{Th}(\text{NO}_3)_4$  feed solutions and changes in atomizing-nozzle conditions. The particle size increased when the reflector temperatures were decreased from 1600 to 1000°C, but decreasing to 600°C did not give any significant additional increase. Doubling the feed concentration of the mixed nitrate salts gave larger particles, with a mean diameter of 2.9  $\mu$  at 1000°C reflector temperature.

Ceramic-grade thoria with a uniform distribution of particles varying in diameter from < 1 to 7  $\mu$  was prepared by oxalate precipitation and calcination to 800°C. This powder was evaluated by automatic press-fabrication to rounded pellets for pebble-bed blanket studies followed by determination of bulk densities and spouting-bed attrition rates. With 4 to 5 wt % aluminum stearate (3.4% aluminum) used as a binder, 4000 to 5000 psi granulation pressures, green-pressed densities of 4.5 to 4.9 g/cc, and 1750°C firing for 4 hr, densities of 9.5 to 9.7 g/cc and attrition rates as low as 0.21 wt % per hour were obtained. When 1% Carbowax was used as a binder, a density of 8.7 g/cc and 0.31 wt % per hour attrition rate were obtained with blends of 70% 950°C-fired and 30% 800°C-fired powder, a granulation pressure of 7500 psi, a green density of 5.0 g/cc, and calcination at 1750°C for 4 hr.

Increasing the calcination temperature for  $\text{ThO}_2$  pellets from 1300 to 1750°C increased the density 10% and lowered attrition losses by a factor of 2.

Reactor Analysis. - The possibility of a criticality accident in transferring irradiated fuel solution from the HRT was investigated. The transfer vessel is cylindrical, with a diameter of 19-1/4 in. and a height of 30-1/2

in. and is shielded with 9 in. of lead. It will be loaded with 100 liters of fluid containing 8 kg of enriched uranium in an aqueous solution (25%  $D_2O$ -75%  $H_2O$ ); 250 g of gadolinium will be present for neutron poisoning. The infinite multiplication constant is less than unity when the fuel is uniformly dispersed. Settling of the uranium would increase reactivity but would not cause the effective multiplication constant to exceed 0.86.

Homogeneous Reactor Instrumentation. - A stem-sealing bellows assembly was developed by Fulton Sylphon Division, Robertshaw-Fulton Controls Company, for use as a replacement for the Clifford Manufacturing Company bellows which failed in service in the HRT-sampler isolation chamber.

Life tests were performed on five Fulton Sylphon bellows test assemblies with 1000 psig applied externally at 225°C. Four of the units were stroked 1/8 in., with 50% of the stroke in extension and 50% of the stroke in compression. Average life of the four units was 3950 strokes. The fifth assembly exhibited a life of 55,160 strokes when tested in a similar manner with a stroke length of 1/16 in. The 1/16-in. stroke length corresponds to that used in the HRT isolation chamber.

The instrument and control system of the LITR HB-2 in-pile test loop was revised and upgraded as required by conversion of the loop from solution to slurry and as required for conformance with present standard practices for experiment safety systems.

Revisions were made to the HRT instrumentation and controls system to provide for containment of steam within the reactor cell in the event of rupture of a heat exchanger tube with subsequent leakage of the steam safety block valves. Revisions were also made to prevent release of radioactive materials through the cell jet line.

Metallurgy and Ceramics. - New ultrasonic measurements of the HRT core-vessel thickness were made as part of the remote-maintenance operations following run 21. The remote manipulator and techniques (immerscope) were the same as those used after run 20. The only major change was an improvement in the data processing techniques. The sources of error in the measurements were the same as before and resulted in a total error somewhat less than 4%.

Measurements were made at about 30° intervals of longitude and 20° intervals of latitude. The relative longitudinal positions of these measurements and those after run 20 and the original measurements made at Newport News are not known. Nevertheless, comparisons made at various latitudes are meaningful since there is little variation in thickness along any one latitude for any particular set of measurements.

Such a latitude-by-latitude comparison of thickness between the original measurements and those made after runs 20 and 21 was made, where each point represents the average of 15 to 25 individual measurements.

The thickness of the core tank in the region from the top of the core to 110° (20° below the equator) has been reduced approximately 14 mils since the core was installed. Between this latitude and that of the top screen (135°) the reduction in thickness is greater and increases as the screens are approached. At the latitude 130° the thickness has been reduced by about 35 mils. It should be noted that the roughness of the inside of the vessel below 110° makes measuring very difficult, and only seven interpretable measurements were made at 135°.

The thinnest spot measured was 0.250 in. at a point just above the top screen. This was probably not the thinnest spot on the vessel, however, since measurements could not be made in the bottom of pits or in very rough areas.

Out-of-Pile Solution Corrosion Tests. - Dynamic corrosion tests were conducted to determine the corrosion of stainless steel in uranyl sulfate solutions containing higher free-acid concentrations than had previously been tested. Type 347 stainless steel specimens were exposed to a solution containing 0.04 m  $\text{UO}_2\text{SO}_4$ , 0.025 m  $\text{CuSO}_4$ , and 0.05 m  $\text{H}_2\text{SO}_4$ . With no pretreatment a critical velocity of about 10 fps was observed, and even at this low velocity about 0.002 in. of metal corroded before a protective film formed. Exposure of specimens to oxygenated water at 280°C for 48 hr prior to exposure to the uranyl sulfate solution at 250°C for 270 hr resulted in a critical velocity of 15 to 20 fps; at flow rates less than the critical velocity about 0.001 in. of metal corroded during formation of the protective film. When specimens were given the above pretreatment and exposed to the uranyl sulfate solution at 300°C for 319 hr, a critical velocity of 45 to 50 fps was observed and only 0.0001 to 0.0003 in. of metal corroded at flow rates less than the critical velocity. The same specimens exposed at 300°C (without descaling) were then exposed to the uranyl sulfate solution at 250°C for 560 hr, during which time no further corrosion occurred up to 50 fps.

The above experiments indicate that pretreatment can be beneficial for relatively short periods of time. However, it must be realized that films developed in a system with a high critical velocity are metastable when exposed at flow rates above the critical velocity in a different system. Thus, although the specimens exposed at 300°C resisted attack when exposed above the critical velocity at 250°C, it would be expected that the protective film would eventually deteriorate at velocities much above 10 fps, with a resultant high corrosion rate of the steel. How long the temporary protection would last cannot be predicted.

In-Pile Solution Corrosion Tests. - Zircaloy-2 specimens from the first ORR in-pile solution loop were examined for weight loss, induced activity, and composition of materials retained on specimen surfaces. This experiment, O-1-25, employed a  $\text{D}_2\text{O}$  solution 0.04 m in  $\text{UO}_2\text{SO}_4$ , 0.016-0.036 m in  $\text{H}_2\text{SO}_4$ , and 0.006 m in  $\text{CuSO}_4$ ; the temperature was 280°C. The Zircaloy-2 specimens were taken from stock fabricated according to Picklesimer's specifications, and the Zircaloy-2 as well as other zirconium-alloy specimens were chemically polished.

The induced-activity results show that at the reactor power of 16 Mw the neutron fluxes on specimens ranged from  $2 \times 10^{13}$  to  $10^{12}$  neutrons  $\text{cm}^{-2}$   $\text{sec}^{-1}$ , and the calculated solution power density ranged from 6.6 to 0.3 w/ml. These maximum values are greater than those experienced in the LITR HB-2 facility by a factor of about 1.5.

The Zircaloy-2 weight results were analyzed on the assumption that the relationship of corrosion rate, R, to power density, P, was the same as that found for Zircaloy-2 in previous loop and autoclave experiments which, in general, employed  $\text{H}_2\text{O}$  solutions, Zircaloy-2 specimens with machined surfaces, and specimen material from stock fabricated to give preferred grain orientations. The previously determined relationship is given in the following equation:

$$\frac{1}{R} = \frac{2.3}{P\alpha} + \frac{1}{K} ,$$

where  $\alpha$  represents the effect of sorbed uranium on the fission-recoil intensity near the surface, and  $K$  is constant for a given temperature and is evaluated by extrapolation of the corrosion data to infinite power density. The value of  $K$  determined for the present results is about the same (40 mils/yr) as that determined for the different type material, surface preparations, and solutions in the previous experiments. The indicated values of  $\alpha$  are somewhat greater than those expected from the previous results; for example, for some specimens exposed to an average velocity of about 1.5 fps, the average value of  $\alpha$  was 7.8, compared with a value of 6 to 7 determined previously for similar type specimens and solution concentrations and at a velocity of  $\sim 0.8$  fps. The higher  $\alpha$  values in the present experiment may have been due to a low hydrogen ion concentration at temperature (a result of a greater than usual rate of steel corrosion). The amounts of uranium found on specimen surfaces by chemical analyses are considered to be in reasonable agreement with the  $\alpha$  values determined from the corrosion results.

The results obtained with specimens having different ratios of exposed to covered areas clearly show that corrosion on the covered surfaces was greater than that on the exposed. The indicated  $\alpha$  value for the covered surfaces is between 8 and 11; values for the surfaces exposed to different solution velocities range between 2 and 6.

The results for two specimens of crystal-bar zirconium indicate a  $K$  value of about 20 mils/yr for this material, a value in near agreement with that previously determined. The indicated  $\alpha$  value is about 1.5 times greater than that for similarly located Zircaloy-2 specimens.

Specimens of Zr-15Nb, Zr-15Nb-2Mo, and Zr-15Nb-1Cu in the  $\beta$ -quenched condition show better corrosion resistance than Zircaloy-2. However, specimens of these materials heat-treated at 400 to 500°C for one to two weeks showed poorer corrosion resistance than the Zircaloy-2.

Supporting Radiation Corrosion Studies. - The apparatus for the electrochemical measurement of corrosion rates in aqueous solutions at elevated temperatures (200-300°C) was modified to permit the temperature of the Teflon seals to be held near 25°C while the system was operated at high temperatures. It has been used in measurements of Zircaloy-2 corrosion in the temperature range 250 to 300°C in solutions of oxygenated 0.05  $\underline{m}$  H<sub>2</sub>SO<sub>4</sub>. The seal performs satisfactorily, but some difficulties have been encountered in the contact between the zirconium lead wire and the Zircaloy-2 specimens. The latest measurement, in which the zirconium lead wire was Heliarc-welded to a machined tip on the specimen, gave the best results, but here also there is some question in the interpretation of the results because the rate on the welded areas was apparently higher than on the other areas (white oxide was formed). In this experiment, which was at 258°C, the rate-time results for the first 2000 min can be expressed by an equation of the form:  $1/R = 1/A + Bt$ , where  $R$  is the corrosion rate in  $\mu\text{g}$  of O<sub>2</sub> per cm<sup>2</sup>-min,  $A$  is the initial rate (not adequately established by the data),  $B$  is a constant equal to 0.4 cm<sup>2</sup> per  $\mu\text{g}$  of O<sub>2</sub>, and  $t$  is the time in minutes. An initial rate of 0.4  $\mu\text{g}$  of O<sub>2</sub> per cm<sup>2</sup>-min (40 mils/yr) was obtained at 3.7 min. Conformance to this equation shows that logarithmic kinetics are obeyed. From 2000 to

3600 min the rate decreased to a steady-state rate of about 0.15 mil/yr and remained constant until the experiment was terminated at 18,000 min.

The area of the welded section which exhibited the white oxide was 0.06 cm<sup>2</sup> or about 1% of the total area. Its contribution to the total corrosion current for the major portion of the experiment is probably negligible. However, at the steady state it is conceivable that the welded section could have been carrying a significant part of the corrosion current.

In-Pile Blanket Materials Tests. - The 5-gpm in-pile slurry loop was installed in beam hole HB-2 of the LITR, and in-pile operation was begun on July 19. The loop is charged with thorium oxide slurry to a concentration of 1350 g of Th per kg of D<sub>2</sub>O and contains 0.5 wt % enriched uranium, based on thorium, and palladium catalyst for recombination of radiolytic gas. Temperature of the circulating slurry is 280°C, and an oxygen atmosphere is maintained in the system.

Loop operation appears satisfactory with regard to circulation of the slurry for the 50 hr of operation to date with the reactor at 3 Mw. The palladium catalyst activity has been adequate in maintaining the partial pressure of radiolytic gas at 10 psi during this period.

A sintered-metal filter located in the loop main stream provides thoria-free filtrate for the pressurizer feed stream and a pump-bearing purge to prevent entry and accumulation of thoria in these regions. The flow rate through the pressurizer and pump-bearing region (connected in series) decreased substantially during the initial 24 hr of irradiation (from 3.8 to 0.9 cc/sec), but this rate of decrease was not continued and operation of the loop has not been affected.

## MOLTEN-SALT REACTOR PROJECT

Component Development. - A 1/5-scale plastic model hydrodynamically similar to the MSRE core vessel has been designed to be operated with 45°C water at reactor velocities that give the same Reynolds number and pressure gradients as those in the reactor. The inlet volute, the core-wall cooling annulus, and the bottom head of the vessel will be simulated, but the graphite lattice will be represented by an orifice plate that will produce the equivalent pressure drop. It is planned that this model will be in operation early in August.

Design for a full-scale model hydrodynamically similar to the reactor was started. The selection of a test fluid with a kinematic viscosity identical to that of the molten salt will be made. The most likely possibilities are glycerol and Karo solutions. The 1/5-scale model results will be used to guide the final design of the full-scale model.

A preliminary flowsheet was prepared for a recirculating purge-gas system which includes provisions for emergency once-through use and disposal through an off-gas system. Tentative specifications for the oxygen removal equipment are being prepared to permit the initiation of work on this component.

A design for a freeze valve was started. A rig for testing this and other valve designs is being constructed, and the test should begin by the end of August.

A loop for testing freeze flanges was designed, and construction was started. The two flanges to be tested initially are a 4-in. flange which has been thoroughly analyzed for thermal stress, and a more recently designed 3-1/2-in. flange which is available. These flanges are connected in series in the loop and are to be examined for thermal-cycle endurance, cooling requirements, and gas-seal problems. This test should be started by the first of September. A "best" design based on thermal-stress analysis and the gas-sealing capability will be completed and fabrication started in August.

Preliminary studies of a system mockup for an enricher-sampler test are being prepared for component sizing, system layout, and design. It is planned that this will be an all-INOR-8 loop, including all pump parts which are in contact with the salt. A study showed that there are no problems in locating the loop in Building 9204-1.

Remote Maintenance. - The maintenance mockup will be reactivated during August to supply training and to permit the obtainment of preliminary data on freeze flanges and heaters.

Chemistry. - The secondary coolant for the MSRE is  $\text{Li}^7\text{F}-\text{BeF}_2$  (66-34 mole %); this mixture, which approximates closely the composition of the compound  $\text{Li}_2\text{BeF}_4$ , melts at  $465^\circ\text{C}$  and has a normal boiling point of about  $1450^\circ\text{C}$ . At  $550^\circ\text{C}$ , the temperature at the exit of the radiator, the density of the coolant is  $1.96 \text{ g/cm}^3$  and the viscosity is 10 centipoises. The choice of 66 mole % LiF was influenced by the fact that at this point in the LiF- $\text{BeF}_2$  binary system melting points increase about  $25^\circ\text{C}$  per mole % in the direction of increasing LiF, while viscosities, at heat-exchanger temperatures, increase about 1 centipoise per mole % in the direction of increasing  $\text{BeF}_2$ . Also, a coolant with a melting point higher than that of the fuel ( $450^\circ\text{C}$ ) provides a safeguard against inadvertent freezing of the fuel.

The concentration of  $\text{UF}_4$  in the MSRE fuel is to be adjusted by additions of a binary eutectic melt,  $\text{Li}^7\text{F}-\text{UF}_4$  (73-27 mole %; melting point  $490^\circ\text{C}$ ), to a carrier which is  $\text{Li}^7\text{F}-\text{BeF}_2-\text{ThF}_4$  (64.75-31.1-4.15 mole %). The phase behavior of the compositions throughout the range from pure additive to pure carrier has been established by the characterization of samples which were quenched after equilibration in the vicinity of the melting point. No increase in the melting point ( $450^\circ\text{C}$ ) occurred for combinations containing as much as 11 mole %  $\text{UF}_4$ , and larger proportions of additive gave increases which were approximately linear with the mole %  $\text{UF}_4$  in the resulting mixture. The initial phases which precipitate on cooling the quaternary mixtures contained smaller U/Th ratios than the melts from which they precipitated, which is favorable with respect to the chances of inadvertently segregating uranium-rich phases by partial freezing during startup or replenishment.

Metallurgy. - An unsintered molybdenum fiber compact was impregnated with Au-Cu by induction heating in hydrogen as part of a program to develop a solidified metal seal. Although the impregnation operation seemed successful, a leak-tight seal was not made between the compact and two molybdenum plates. Attempts are being made to remedy the situation by compressing the seal when the alloy is molten and by closer control of the seal geometry.

Procedures are being developed for making the tube-to-header joints of the MSRE heat exchanger by the welded and back-brazed technique. Six sample

inert-arc welds of 1/2-in.-OD, 0.045-in.-wall INOR-8 tubes to 1-1/2-in.-thick INOR-8 plate were made by using various currents and torch travel speeds. Metallographic examination of these welds indicated that weld penetration of about 1-1/2 t (t = 0.045 in.) or about 67 mils could readily be obtained by utilization of trepanned joints.

A series of six precipitation tests was made with AGOT graphite and LiF-BeF<sub>2</sub>-UF<sub>4</sub> (62-37-1 mole %) in which only the volume of the graphite was varied in order to determine the relationship of graphite volume to uranium precipitated. The test conditions and results are summarized below. Chemical analyses were used to determine the quantity of uranium that precipitated as UO<sub>2</sub>. The uranium precipitated per cubic centimeter of bulk volume of the graphite averaged 1.3 mg. It was assumed in these tests that the volume of salt and the area of graphite in contact with the fuel do not affect the quantity of precipitate that occurs. Past data for volume ratios of graphite to fuel in the range of these tests support these assumptions.

Ratio of Graphite Volume to Fuel Volume	Weight of U Precipitation	
	Total (mg)	Per Unit Volume of Graphite (mg/cc)
5:1	3.4	0.97
10:1	8.3	1.2
15:1	17.7	1.7
20:1	20.2	1.4
27:1	20.3	1.1

(1300°F, 100 hr, vacuum)

Corrosion Tests. - The third and final hot-leg insert was removed from INOR-8 forced-convection loop 9354-4 following the completion of 15,140 hr of loop operation. As previously discussed (ORNL-2890, p 35-40), three inserts were installed at the end of the hot-leg section of the loop to provide data on the weight changes resulting from INOR-8 in contact with a beryllium-base fluoride fuel mixture. The inserts were scheduled to be removed after 5000, 10,000, and 15,000 hr of exposure respectively. The loop began operation in July 1958, under the conditions shown below:

Salt mixture	LiF-BeF <sub>2</sub> -UF <sub>4</sub> (62-37-1 mole %)
Maximum fuel-metal interface temperature	1300°F
Minimum salt temperature	1100°F
ΔT	200°F
Reynolds number	1600
Flow rate	2 gpm

Examination of the third insert indicates that an average weight loss of 1.7 (±6%) mg/cm<sup>2</sup> occurred along its 4-in. length. If uniform removal of

the surface metal is assumed, this weight loss corresponds to a loss in wall thickness of 0.08 ( $\pm 6\%$ ) mil. The first two inserts removed after 5000 and 10,000 hr showed weight losses of 1.8 ( $\pm 2\%$ ) and 2.1 ( $\pm 3\%$ ) mg/cm<sup>2</sup> respectively. Again, assuming uniform removal of the surface metal, these weight losses correspond to respective losses in wall thickness of 0.08 and 0.09 mil. On all three inserts, no detectable loss in wall thickness was noted in comparing micrometer measurements of the inserts taken before or after test, and no attack was revealed in metallographic examinations.

Reactor Analysis. - Preliminary criticality and gamma-heating calculations were completed for the MSRE. The calculated critical loading for a reactor with a cylindrical core 54 in. in diameter and 66 in. high was 0.76 mole % enriched uranium (93.3% U<sup>235</sup>); this gives a critical mass (in the core) of 16 kg. At a reactor power of 5 Mw the peak power density in the core (assuming the core to be a homogeneous mixture of graphite and fuel salt) is 5 w/cm<sup>3</sup>; the average power density is 2 w/cm<sup>3</sup>. Gamma heating produces a power density of 0.1 w/cm<sup>3</sup> in the core wall at the midplane and 0.2 w/cm<sup>3</sup> in the support grid at the bottom of the core at the reactor center line.

Estimates have been made of the heat generation rate in the pump-bowl gas space due to gaseous fission products and their descendants. If the descendants behave as gases and are removed by the sweep gas, the heat generation in the gas space is reduced in comparison with the heat generation if the descendants stick to the walls of the gas space. For a purge flow rate of 50 gpm and a sweep rate of 1000 liters of helium per day, the heat generation rate is 8.0 kw if all the descendants stick to the wall, and 6.5 kw if the descendants behave as gases.

Calculations have been done to estimate the xenon stripping for various purge rates. The equilibrium Xe<sup>135</sup> poison fraction (i.e., ratio of xenon thermal macroscopic absorption cross section to fuel thermal macroscopic fission cross section) is reduced from 0.05 to 0.01 by a purge rate of 1% of the system flow rate.

Thorium-Breeder-Reactor Evaluation Studies. - The nuclear and fuel-cost performances of aqueous homogeneous (AHBR), molten-salt (MSBR), liquid-bismuth (LBHR), gas-cooled graphite-moderated (GGBR), and gas-cooled heavy-water-moderated (GWBR) breeder reactors were evaluated. For each system a net electrical plant capability of 1000 Mw was considered; on-site processing of the fuel and fertile streams under equilibrium conditions was assumed. The maximum annual fuel yields of the above reactors were 16, 8, 4, 4, and 4%, respectively, at fuel cycle costs of 1.2, 1.0, 1.3, 1.5, and 1.6 mills/kwhr. The respective minimum fuel cycle costs were 0.9, 0.6, 1.0, 1.2, and 1.3 mills/kwhr at fuel yields of 8, 4, 2, 2, and 2% per year.

The development effort required to achieve successful reactor operation was estimated to be about the same for the AHBR and MSBR, and several times as much for the other systems. Consideration of probable maximum errors in nuclear data of U<sup>233</sup> had small effect on the estimated performance of the AHBR, but reduced the maximum fuel yields in the MSBR by about half and raised the minimum fuel cycle cost about 0.3 mill/kwhr.

MSRE Design. - The MSRE design effort is now organized in five categories: facilities, components, system layout, instrumentation, and analysis.

All phases of design are now being prosecuted, and the progress is sufficient to keep the project on schedule.

Component designs are now being stress-analyzed for the purpose of establishing final dimensions and tolerances.

Layout of components in the cell has been facilitated by the decision to remove drain tanks from the reactor compartment while maintaining them within the primary containment area. Layouts of both primary and secondary salt circuits are currently being stress-analyzed.

Gas-handling equipment has been investigated only to the extent of a preliminary flowsheet. Instrumentation requirements are partially defined, but no system design has been started.

Studies of drain-tank cooling, sampling and enriching, electrical heating, remote maintenance, and shielding have been started.

A preliminary layout of the MSRE primary pump was completed and reviewed. Design of a water test for this pump was started. INOR-8 castings of the impeller and volute are being procured. Computations of equilibrium temperatures in the pump-tank wall and other gas-immersed structures inside the pump tank are nearly complete.

#### HIGH FLUX ISOTOPE REACTOR

Reactor Physics Calculations. - Further calculations have been made in connection with the HFIR island void coefficient of reactivity. Previous calculations indicated that an optimum-size void (45% of island volume) in an all-water island would result in a 2.5% increase in  $k$ . However, with the 200-g plutonium target in the island the corresponding maximum change in  $k$  is reduced to about 1%, and somewhat larger targets, which would increase the production of  $\text{Cf}^{252}$  to some extent, could reduce the maximum change in  $k$  to less than one dollar. Although the HFIR has been designed primarily for the production of transplutonium isotopes, in which case the above target must be used in the island, there may occasionally be times when it is desirable to insert only a very small target in the island for the purpose of obtaining the maximum possible flux. Calculations have been made in connection with this case to determine how much and what kind of solid material (permanent voids) must be inserted in the island to limit the maximum change in  $k$  due to real voids to certain specified values, and to determine how much the fluxes in the island are reduced. The results indicate that for a particular maximum change in  $k$  the material with the highest moderating ratio results in the smallest decrease in peak thermal flux. For example, if a maximum reactivity addition of one dollar is specified, the use of beryllium (no  $\text{Li}^6$  poison) will reduce the peak thermal flux by 13%, as compared with 27% for aluminum. Beryllium, however, is subject to an increase in its absorption cross section as a result of  $\text{Li}^6$  buildup. For the HFIR the concentration of  $\text{Li}^6$  nearly reaches a maximum by the end of 0.2 yr; the corresponding additional decrease in peak flux is about 5%, making a total of 18%.

Heat Transfer. - An extensive evaluation of the Zenkevich-Subbotin burnout correlation with all available data (approximately 550 burnout tests of both U.S. and Soviet origin) indicates that the over-all agreement is best

in the pressure range  $600 < P < 3085$  psia. Within the pressure range  $14 < P < 600$  psia, the agreement between prediction and experiment becomes increasingly poor as pressure decreases. It is not known whether this divergence is caused by greater experimental inaccuracies, a change in the mechanism of the boiling process, or simply a failure of the correlation equation. Agreement of ORNL HFIR burnout data with predicted values at pressures of 350 to 570 psia has been excellent.

Preparation of an ORNL report on prediction of natural-circulation burnout with low-pressure water is continuing. A final burnout determination with a test section simulating the ORR geometry has revealed that the general prediction method which has been developed adequately takes into account such factors as hot spots with double the average heat flux, unheated terminal flow-channel extensions, and highly restricted liquid recirculation paths.

Photomicrographs of the interior surface of an aluminum test section which was fitted with an unbonded, axially oriented stainless steel spacer strip and tested to burnout show that considerable surface corrosion and pitting took place. Whether the attack was caused by galvanic action, concentration cells, or fretting is unknown at this time.

Critical Experiments. - Another set of critical concentrations of the solutions comprising the preliminary critical assembly supporting the HFIR has been established. In this case the fuel annulus contained uranyl nitrate at a  $U^{235}$  concentration of 105.9 g/liter in an  $H_2O-D_2O$  solvent of 70.1 at. % D; the specific gravity was 1.2262. The inner reflector annulus was a  $D_2O$  solution of 2.35 g of natural boron per liter. As before, natural water filled both the central cylindrical region and the outermost annular reflector. Fission rate distributions have been measured with bare and cadmium-covered chambers.

Corrosion. - Three tests to determine the effect of heat flux on the corrosion of type 6061 aluminum by water have been completed. In all cases the heat flux was  $1.6 \times 10^6$  Btu  $hr^{-1}$   $ft^{-2}$ , the pH of the water was 5 ( $HNO_3$ ), and the duration was ten days. As the tests progressed the formation of a layer of corrosion products on the heat transfer surface caused a gradual linear increase in the temperature of the aluminum. It is presumed that the rate of temperature increase is proportional to the corrosion rate.

In one test the velocity of the coolant was 34 fps and the temperature of the water at the outlet of the specimen was 190°F; the observed rate of temperature increase was 4 to 5°F per day, essentially the same as the rate observed with type 1100 aluminum under the same conditions. In another test the conditions were the same except that the outlet water temperature was maintained at 175°F. The rate of temperature rise was approximately 0.4°F per day, indicating a very low corrosion rate for the aluminum. This latter experiment demonstrates the importance of temperature on the corrosion of aluminum. The third run was made with a coolant flow rate of 48 fps and an outlet water temperature of 190°F. During the ten-day experiment the maximum rate of temperature increase was 3°F per day.

Although the type of specimen currently in use does not allow a precise measure of the extent of attack, the corrosion damage in all three cases appeared to be very slight. All specimens were covered with a thin, nearly transparent oxide, and no evidence of film stripping or localized attack was

apparent. Attempts are being made to fabricate a specimen from which accurate corrosion data can be obtained.

Metallurgy: Evaluation of the Mark II-A Test Element. - The mark II-A test element has been subjected to a series of three hydraulic tests at room temperature at calculated flow velocities up to 60 fps. Plate spacing measurements were made following 4- to 6-hr tests at 35 to 40 fps (test No. 1), at 50 fps (test No. 2), and at 60 fps (test No. 3). Summary calculations of the spacing measurements taken after the 40- and 50-fps tests have been made and correlated with similar measurements made on the element in the as-fabricated condition.

Comparison of the three sets of data taken at the three locations, namely, (1) those taken adjacent to the inner tube, (2) those taken near the center of the involute plate, and (3) those taken near the trailing edge of the involute, indicated that the mean values of the measurements in each case were slightly increased as a result of the flow test. However, the variation at each position appeared to be only slightly changed as a result of the hydraulic tests.

It was noted after the testing that one of the fuel plates had partially pulled loose from the inner groove at the water inlet end of the test element. The partially displaced plate did not appear permanently damaged and was easily returned to its normal position. Also at this time the outer tube was removed from the test element for an examination of the band weldments. At the water inlet end of the test element, many of the welds which anchor the trailing edge of the plates to the circumferential bands were cracked. This element was repaired and returned for further testing.

Metallurgy: Fabrication of the Mark II-B Fuel Element. - The fuel plates for the full-sized inner and outer annulus of the mark II-B element to be completed in September will have a  $0.050 \times 0.345 \times 22.0$  in. long spacer rib attached near the trailing edge of the involute curvature. Both resistance spot-welding and ultrasonic spot-welding techniques have been investigated for the purpose of attaching these spacers. Satisfactory resistance spot-welding parameters have been established. In view of the tight schedule for the mark II-B element, the utilization of an ultrasonic welding technique for spacer rib attachment does not appear to be practical at this time.

A new forming die has been constructed to accommodate the 22-in.-long plate required by the present mark II design, and this die has been used to form 12 of the 40-mil-thick aluminum (type 6061-0) dummy fuel plates. Measurements of these plates indicate the straightness of the formed plates to be within 2 mils of flatness (with a deviation from the true involute of approximately  $\pm 6$  mils). Duplication of the 12 plates indicates a maximum spread of 10 mils. In view of the present water channel tolerances, plates fabricated with this die should be satisfactory.

Chemical analysis of the first vacuum-melted 30% U-2% Si-0.05% Al casting indicated a 35% loss in boron charged. It is suspected that a loss of this magnitude may be due to evaporation of boron during vacuum-induction melting. To substantiate this thesis, two melts were prepared, one under a vacuum of 1 to 3  $\mu$ , the other under argon at 5 psi. The castings were extruded using a 16-to-1 reduction in area, and samples are being analyzed chemically.

Microscopic examination of sections of this silicon-modified casting revealed primary  $UAl_3$  in a eutectic matrix. The  $510^\circ C$  soaking period prior to extrusion appears to spheroidize the eutectic structure. Examination of sections from extruded rod revealed that the crystallites of the  $UAl_3$  are finer adjacent to the surface and increase in size in the center region of the rod.

A series of 15 composite fuel plates for the mark II-B fuel element was fabricated. Nine plates were of the inner annulus variety, which is characterized by a 1:4 gradient in radial fuel concentration. The remaining six were of the outer annulus variety, which has a 2:1 radial fuel concentration gradient. Single and double aluminum-clad type 6061 aluminum alloy served as the cover plate and frame stock. A 30 wt % U-2 wt % Si-0.05 wt % natural B-bal Al alloy was employed as the active core material, and inserts were composed of type 3A aluminum alloy which had been modified by a 0.07 wt % natural boron addition.

After prerolling and roll-cladding at  $450^\circ C$ , a blister test was conducted at  $500^\circ C$ . Only one plate of the 15 blistered in this test. Radiographic examination to qualitatively determine degree of segregation revealed that only one plate showed evidence of segregation.

Design: Fuel Plate Stability. - A creep test rig was designed and fabricated for use in the fuel-element stability studies. An involute fuel plate is clamped around the edges in a carbon-steel frame. The entire assembly is mounted in an oven and held at a temperature of about  $450^\circ F$  for about ten days. This results in a differential expansion which approximates that between the fuel plate and side plates in the reactor operating fuel element. Preliminary results indicate that deformation during operation and the resulting creep are not serious. In later tests a pressure differential will be applied across the plate at temperature to determine the effect of the combined load.

Design: Beryllium Reflector. - The fuel will be surrounded by a 1-ft-thick, 2-ft-high beryllium reflector. The inner 3 in. of this beryllium is designed for easy removal. This inner section is composed of four concentric cylinders separated by 50-mil coolant channels. The outer beryllium is a solid annulus with  $3/16$ -in. coolant holes. The location of the water coolant channels was designed to maintain the thermal stress below 7000 psi in the beryllium.

Design: Shielding of the Reactor Water System. - Calculations for determining the thickness of ordinary concrete required for shielding the primary coolant system were completed.

During normal operation 2 ft of concrete is sufficient for shielding most of the reactor water system; however, the 48-in.-dia decay vessel will require 6 ft of concrete shielding at the reactor discharge end. In the water cleanup system the demineralizers and filters will require up to 4-1/2 ft of concrete.

## MARITIME REACTORS PROGRAM

The second set of swaged  $UO_2$  fuel rods, described previously (ORNL-2960), was removed temporarily from the ORR pressurized-water loop after two operating cycles at 16 Mw to facilitate the modification work on the ORR. A lead and depleted-uranium shield was fabricated and installed to reduce the radiation level from the loop components and the reactor support grid during this work.

## NUCLEAR TECHNOLOGY AND GENERAL SUPPORT

Reactor Evaluation Studies. - Reactivity lifetimes and fuel costs were calculated for several one-region, batch-loaded, homogeneous reactors by use of the computer program Expire. The fuel was assumed to be processed at a central station facility on a batch basis. The reactors considered were 8- and 10-ft-dia spheres fueled with either slightly enriched  $UO_3$  or a mixture of highly enriched  $UO_3$  and  $ThO_2$ . In all cases the reactor thermal power was 150 Mw; the external power removal capability was 20 kw/liter, and the thermal efficiency was 26.6%.

For both reactor diameters and fuel materials, the minimum fuel costs were associated with a fertile material concentration of 200 g/liter. In the 10-ft-dia reactors the optimum ratio of fissionable to fertile atoms was 0.04; the minimum fuel costs were 3.36 and 3.58 mills/kwhr in the  $UO_3$  and  $UO_3$ - $ThO_2$  systems respectively. In the 8-ft-dia reactors the optimum atom ratios were 0.04 and 0.06 for the  $UO_3$  and  $UO_3$ - $ThO_2$  systems respectively; the associated minimum fuel costs were 3.75 and 3.91 mills/kwhr.

Radiation Detector Development. - A theoretical study of the scintillation process in thallium-activated alkali iodides has been continued, with attention directed to the behavior of the scintillation efficiency for particles of very low specific energy loss (electrons). The experimentally observed behavior can be accounted for on the assumption that energy transport, from the wake of the incident particle to the activator sites, takes place via charge-neutral energy carriers formed by the recombination of electron-hole pairs. The incorporation of this effect with the previously studied behavior for heavily ionizing particles permits a description of scintillation efficiency for all charged particles; the over-all features are in agreement with experiment. The theoretical model adopted also permits a description of effects dependent on activator concentration.

The large sodium iodide crystal to be used as the detector in the model IV gamma-ray spectrometer has been delivered to the Bulk Shielding Facility. This crystal is a right circular cylinder, 9 in. in diameter and 12 in. long, and has a 1-in.-dia, 2-in.-deep well centered on one face, into which the gamma rays will be collimated. Before this crystal was delivered, a 5-in.-dia, 5-in.-long sodium iodide crystal was used for testing the spectrometer. The reproducibility of the positioning of the spectrometer was investigated, as well as the use of calibration sources built into the collimator. Several observations of the gamma-ray spectrum of the Pool Critical Assembly were made, primarily to check the reproducibility of the data.

Zirconium Metallurgy. - A metallographic specimen was cut from the wall of the Zircaloy-2 core tank of the HRT at the site of the second (upper) hole, formed at the end of run 21. Metallographic examination of a cross

section of the specimen showed that the hole had been burned through the core wall by an external heat source, presumably a concentration of fissioning uranium. The metal at the edge of the hole had been melted, as was shown by the mixture of oxygen-stabilized  $\alpha$ -zirconium and melt existing in the microstructure. The time cycle of the burning event was very short, about 2 to 5 sec, as was shown by the existence of intermetallic stringers (formed during the commercial fabrication of the plate material) in a matrix that had been  $\beta$  phase at a temperature of at least 1200 to 1300°C. The duplex acicular  $\alpha$  needle structure observed in the microstructure indicated that the cooling rate had been much faster below approximately 850 to 900°C than above that temperature, a circumstance which could have occurred by the collapse of a steam blanket at the site of the hole. The microstructural examination did not show any basis for believing that the core tank had been damaged by anything other than the burning of the two holes in the wall.

Fuel Element Development. - A series of stainless steel tubes, 0.750 in. OD with 0.035-in. wall thickness, was tamp-packed with uranium nitride and densified by swaging at room temperature. Densifications varied from 78.9% of theoretical after 46.7% reduction in area to 83.1% of theoretical after 58.4% reduction in area. This value remained unchanged with increased reductions in area up to 79.6%. The uranium nitride was produced by reaction of uranium chips with nitrogen and contained 7.49 wt %  $N_2$  compared with 5.62 wt %  $N_2$  for stoichiometric UN. X-ray diffraction indicated that this material was contaminated with  $UO_2$  and  $U_2N_3$ .

Investigations of roll-bonding of composite fuel plates with X8001 as the cladding material have revealed that, although bonding of plates appears sound metallographically and gives bond strengths in excess of 9800 psi, blisters form at the bonded periphery of the plates when exposed for seven days in static water at 290°C and 1200 psi. Similarly bonded plates with all edges sealed by inert-arc welding after the roll-cladding process showed no peripheral blister formation when exposed to the test environment.

During development of fabrication techniques for dispersing  $UO_2$  in type 430 stainless steel and roll-cladding into composite plate, it was found that after a 1-hr heat treatment at 1000°C the material became very coarse-grained and susceptible to intergranular attack in 7.5 M  $HNO_3$ . A unique advantage offered by type 430 stainless steel compared with the austenitic variety is the potential of cheaper reprocessing of spent fuel elements by a sensitizing heat treatment and subsequent dissolution in an acid which is compatible with its austenitic stainless steel container.

Preliminary studies indicate that 100% of the uranium is recovered when  $UO_2$ -type 430 sensitized stainless material is dissolved in the 7.5 M  $HNO_3$  solution. Although the dissolution time of 216 hr for a composite plate containing 6.25 g of  $UO_2$  was rather long, a later result showed that the time was reduced 60% when 0.05 M  $HCl$  was added to the 7.5 M  $HNO_3$  solution.

Nondestructive Test Development. - A new ultrasonic technique, complete with instrumentation, has been developed for the measurement of metal thickness. Previous methods involved resonance or pulse-reflection, the time interval between interface reflections being measured by means of the calibrated delay line of an oscilloscope. The new procedure makes use of an electronic counter and a preset counter, in addition to conventional ultrasonic equipment. This permits a digital presentation of the measured metal

thickness. This technique has been used for a survey of wall thickness in the HRT core vessel.

A linear calibration for 7 wt %  $U^{235}$  core blanks has been derived for the gamma spectrometry equipment. Some core blanks containing 13 and 10 wt %  $U^{235}$  have also been analyzed, but calibration is not yet complete.

Inspection development has continued on small-diameter beryllium tubing. Tentative techniques for using radiography, penetrants, resonance and pulse-echo ultrasonics, and encircling-coil eddy currents have been developed. Among the conditions being detected are the presence of high-density material (relative to beryllium), pitting, circumferential and longitudinal cracking, and wall thickness variations.

An eddy-current probe-coil instrument is being developed which can be used to measure cladding thickness and the thickness of thin metal.

Refinements in the spark-discharge-machining technique for producing standard reference notches have increased the accuracy of notch depth reproduction to  $\pm 0.0002$  in., which appears to be the limit with existing equipment.

Mechanical Properties Research. - The relaxation test is being used as a tool to yield quantitative information as to the effects of environment and preferred orientation on the creep properties of Zircaloy-2. The relaxation test data have demonstrated in a relatively short time the influence of orientation on creep strength over a wide range of stress values. The influence of environment on creep strength can be determined as a function of time by use of the relaxation test, again over a wide stress range. It has been shown that air at 900°F strengthens the alloy only after a 10-hr exposure and that the strengthening effect is complete after 400 hr. This type of quantitative information can be used to convert air data directly to inert-environment data or, conversely, inert-environment data to air data, in a manner that can be used easily in design problems.

Materials Compatibility Studies. - A program has been initiated to study compatibility problems involving alkali metals and potential container materials at elevated temperatures. The current interest in the potential utilization of alkali metals as working fluids in reactor-turbine-generator-power systems for space vehicles requires detailed basic and applied studies to resolve the many compatibility problems inherent in these proposed systems. Investigations will be concentrated primarily on potassium, since this metal has many properties which make it attractive for these systems. Basic compatibility studies on lithium, rubidium, and sodium will be included in this program.

Results to date indicate that very little corrosion occurs in the liquid and vapor regions of types 310 and 316 stainless steel capsules in which potassium has been refluxed for time periods of 500 hr at a temperature of 1600°F. Weight-loss data and metallographic examination indicate maximum attack of less than 0.5 mil.

A boiling potassium-type 316 stainless steel loop system was operated at a boiler temperature of 1550°F for 200 hr. A heat balance on the cooler section of the loop was used to determine the mass flow rate (65 g/min) and the vapor flow rate (20 fps) in the system. Metallographic examination and weight-change data revealed a maximum attack of less than 0.5 mil in the system.

A second boiling potassium-type 316 stainless steel loop has been operated for 2600 hr. Test conditions for this loop are: boiler temperature, 1600°F; potassium mass flow rate, 145 g/min; and a vapor velocity of 54 fps.

Fuel Cycle Technology. - Mixed 5% uranium-thorium oxide was densified (1) by partial nitration of mixtures of  $\text{ThO}_2$  and  $\text{UO}_3 \cdot 2\text{H}_2\text{O}$  followed by hydrothermal denitration, or (2) by hydrothermal denitration of the mixed nitrates. After calcination at 1200 to 1300°C, the particle densities of material prepared by the two methods were 98 to 99% of theoretical for calcination in hydrogen and 96 to 98% of theoretical for calcination in air. Samples of these oxides were pneumatically vibrated in stainless steel tubes to bulk densities of 82 to 83% of theoretical. For 10% uranium-thorium oxides prepared in the same way and calcined at 850 to 1250°C, particle densities were about 3% greater for material fired in air than for material fired in hydrogen, and increased linearly from 93.4 to 98.3% and from 91.2 to 95.3% of theoretical, respectively, for the two methods of preparation.

The densities of mixed oxides ( $\text{ThO}_2$ -3.4 wt %  $\text{UO}_2$  arc-fused) vibratorily compacted into tubes with a single-impact-piston pneumatic vibrator showed small differences for varying tube materials, lengths, and diameters, and with the use of a multiple tube assembly. Densities in 6- to 8-ft-long tubes were 8.7 g/cc for two 3/8-in.-OD stainless steel tubes, 8.6 g/cc for two 3/8-in.-OD aluminum tubes, and 8.5 g/cc for 3/4-in.-OD Zircaloy-2 tubes. Densities were 8.77 g/cc in 2-ft-long stainless steel tubes and 8.58 g/cc in aluminum. The density with a rigid bundle of seven 1/4-in.-dia tubes was 8.6 g/cc.

At least two forms of nitrate complex with  $\text{ThO}_2$  were indicated in a thermogravimetric study of dried thoria gels prepared by nitration of  $\text{ThO}_2$ . One is thermally decomposed at about 150°C, and the other is stable at 250 to 340°C, depending on the temperature at which the oxide was nitrated (95 or 170°C).

Power Reactor Fuel Processing: Darex-Thorex Process. - When unirradiated Consolidated Edison  $\text{ThO}_2$ - $\text{UO}_2$  pellets were treated with Darex decladding solution in air, the uranium loss for a 3-hr contact was three times that when air was excluded; the loss rate in air after 3 hr was 0.05% per hour. In the absence of air no increase in loss resulted when the dissolution was done in a 1-w/liter  $\text{Co}^{60}$  gamma-ray field.

The rate of dissolution of  $\text{ThO}_2$ - $\text{UO}_2$  in 13 M  $\text{HNO}_3$ -0.04 M NaF-0.1 M  $\text{Al}(\text{NO}_3)_3$  increased with increasing percentage of the mixed oxide dissolved:

Dissolution (%)	Rate ( $\text{mg g}^{-1} \text{min}^{-1}$ )
0	0.32
1	0.56
60	~ 1.0
80	~ 2.0

The effect of two neutron poisons, boron and cadmium, on the rate of dissolution of high-density 95%  $\text{ThO}_2$ - $\text{UO}_2$  pellets in boiling solutions 13 M in  $\text{HNO}_3$ , 0.04 M in NaF, and 0 to 0.1 M in  $\text{Al}(\text{NO}_3)_3$  was determined. Initial

10-min rates were independent of boric acid concentration up to 0.1 M, but an attempt to prepare, by dissolution, a solution 1 M in thorium and 0.1 M in boric acid resulted in the precipitation of  $\text{Th}(\text{NO}_3)_4$ . As the cadmium concentration was increased from 0 to 0.075 M, the initial 10-min rate in dissolvent containing no aluminum decreased from 2 to 0.7  $\text{mg cm}^{-2} \text{min}^{-1}$ ; in dissolvent 0.1 M in aluminum, the rate increased from 0.7 to 2  $\text{mg cm}^{-2} \text{min}^{-1}$  with the same change in cadmium concentration.

After 48 batch boildowns of adjusted Thorex feed, negligible corrosion was observed on all titanium specimens exposed.

Power Reactor Fuel Processing: Mechanical Processing. - The SRE de-jacketing equipment in Building 3026 was satisfactorily operated by remote control in cold runs. A substitute high-viscosity fire-resistant hydraulic fluid (viscosity 226 sec Saybolt Universal at 100°F) was used in the hydraulically operated multipurpose saw to correct the malfunction which resulted from the use of Ucon Hydrolube AC, a low-viscosity fluid (58 sec Saybolt Universal at 100°F). The  $\text{CO}_2$  fire-fighting system also operated satisfactorily. The cell temperature was decreased from 80°F to 24°F during the first minute of gas release.

A 3-ft section of a stainless-steel-clad porcelain Yankee prototype sub-assembly (thirty-six 0.336-in.-dia tubes) fabricated with Kanigen-brazed diffusion-bonded joints was sheared successfully with an M-shaped punch and 90° anvil. At one of the two ferrule locations sheared, five two-tube pieces and one five-tube piece were produced in a 1-in.-long cut. Under the same conditions, only one two-tube piece was produced in the shearing of a mark I prototype assembly brazed with Nicrobraz alloy (thirty-six 0.5-in.-dia tubes).

In a leaching test, 7.5 kg of sheared stainless-steel-clad  $\text{UO}_2$  fuel (50% fines) was suddenly brought into contact with boiling 13 M  $\text{HNO}_3$ . Foaming was violent, the foam volume exceeding the dissolvent volume. At the end of this test, 12 g (0.16% of the 7.5-kg charge) of flocculent residue (tap density 0.44 g/cc) repeatedly plugged a 0.5-in.-dia gravity outlet drain for the 50°C uranyl nitrate product.

Power Reactor Fuel Processing: Criticality Control. - Use of high-boron-glass packing is being considered as a method of criticality control in conventional tanks. Tests were made in order to determine whether the mixing characteristics were adversely affected by the presence of the packing. Homogeneity determinations with an electrical conductivity probe indicated that the time required for complete mixing varied inversely with the volume of the solution in a tank packed with 1.5-in.-dia  $\times$  1.75-in.-long glass Raschig rings. The times were 23 min for 85 gal and 7 min for 150 gal when air was supplied to the peripheral sparge ring at a rate of 0.5 scfm/ft<sup>2</sup>. The diameter of the tank was 32 in. and the height varied; for a 150-gal volume the height was 60 in. and the draft tubes were submerged approximately 2 in.

Power Reactor Fuel Processing: Solvent Extraction. - An Acid Thorex flowsheet in which a 30% solution of tributyl phosphate (TBP) is used for recovery of uranium and thorium from Consolidated Edison-type fuel was successfully demonstrated on unirradiated fuel solution in a three-column cascade consisting of extraction-scrub, partitioning, and uranium-stripping columns. The total losses of both uranium and thorium were less than 0.1%.

The flow capacity of the pulsed columns was limited by flooding in the top section of the partitioning column ( $750 \text{ gal ft}^{-2} \text{ hr}^{-1}$  at 1 in. amplitude and 50 cycles/min). A flowsheet in which the uranium product refluxes into the line connecting the partitioning and stripping columns and is withdrawn at that point increased the uranium product concentration by a factor of 2 over that obtained without reflux.

Irradiation of synthetic Consolidated Edison fuel solution to 5 and 10 whr/liter with  $\text{Co}^{60}$  gamma rays resulted in about 50% decrease in decontamination with the Acid Thorex flowsheet. After irradiation to 60 and 165 whr/liter the decontamination factor improved by factors of 2 and 5 respectively. Decreasing the TBP concentration from 15 to 5% in the final uranium purification cycle at a uranium saturation of 65% increased the decontamination from fission products by a factor of 2. The decontamination factor decreased by a factor of 5, however, on further decrease of TBP concentration to 2.5% at a uranium saturation of 38%. This indicates a stronger dependence on saturation than on TBP concentration.

#### Power Reactor Fuel Processing: Processes for Graphite-Containing Fuels.

- Prototype Pebble Bed Reactor fuels in the form of 1.5-in.-dia spheres (graphitized and ungraphitized, admixture type) were disintegrated to -10 mesh powder by treating with 90%  $\text{HNO}_3$  either at  $25^\circ\text{C}$  or at boiling. The graphitized specimens disintegrated more rapidly than the ungraphitized, and the outer layers of both fuels disintegrated more rapidly than the central core. About 84% of the graphitized fuel disintegrated in 7 hr, but 24 hr was required for complete disintegration; 65% of the ungraphitized fuel disintegrated in 7 hr, but only about 95% after 24 hr. The powder was removed from the reaction mixture after 6 to 10 hr to avoid the formation of very fine particles which were difficult to filter. After partially disintegrated material had been washed with water, no further disintegration occurred upon subsequent treatment with 90% acid. Two leaches of the powder with 90%  $\text{HNO}_3$  and thorough washing with either water or  $\text{HNO}_3$  resulted in recovery of 99% or more of the uranium. When complete disintegration was not achieved, only 30% of the uranium was leached from the core. Grinding the Pebble Bed Reactor fuels to -4 +8 mesh and leaching with boiling 70% acid recovered only 97.6% of the uranium.

Grinding of an Si-SiC-coated ungraphitized prototype fuel sample to -200 mesh and leaching with 70%  $\text{HNO}_3$ , or grinding to -4 +8 mesh and leaching with 90% acid, recovered 99% of the uranium.

Power Reactor Fuel Processing: Processes for U-Mo Fuels. - Dissolution of U-10% Mo alloy in boiling nitric acid to produce 1 M uranium solutions resulted in precipitation of uranyl molybdates (e.g.,  $\text{UO}_3 \cdot 2\text{MoO}_3$ ) at low acidities, from 1 to 3 M. At acidities greater than 5 M the molybdenum precipitated as  $\text{MoO}_3$ .

Preliminary corrosion tests of titanium-45A in  $\text{HNO}_3$ -0.5 M  $\text{Fe}(\text{NO}_3)_3$  solutions (for dissolution of U-3% Mo cores) showed rates of 0.24 mil/month or less for 72-hr exposures in the range between 3 and 8 M  $\text{HNO}_3$ , but the results were erratic, and some localized attack was observed.

The Zircex process, which involves reaction of fuel cladding and material with anhydrous HCl at  $\sim 500^\circ\text{C}$ , was successfully applied to U-Mo fuel alloy and aluminum cladding. An alloy of 91.6% U-Mo reacted with 10% HCl-90%

air at 400 to 600°C at rates of 8 to 10 mg cm<sup>-2</sup> min<sup>-1</sup> and with chlorine at furnace temperatures above 450°C at a rate of 20 mg cm<sup>-2</sup> min<sup>-1</sup>. Removals of 98 and 90% of the molybdenum were achieved with chlorine and with mixed hydrogen chloride and air respectively. Addition of air to hydrogen chloride doubled the reaction rate and caused removal of over 99% of the chloride from the product. Aluminum reacted with both hydrogen chloride and chlorine at a furnace temperature of 300°C at a rate of 11 mg cm<sup>-2</sup> min<sup>-1</sup>. Stainless steel reacted with chlorine at 600°C at a rate of 0.55 mg cm<sup>-2</sup> min<sup>-1</sup>.

Power Reactor Fuel Processing: Processes for Zirconium-Containing Fuels. - In further corrosion tests, titanium exposed to 0.5 M HBF<sub>4</sub>-HNO<sub>3</sub> corroded at maximum rates varying from 10 mils/month in 3 M HNO<sub>3</sub> in the presence of dissolving zirconium to 295 mils/month in 12 M HNO<sub>3</sub> with no zirconium present.

Power Reactor Fuel Processing: Sulfex Process. - When unirradiated Consolidated Edison ThO<sub>2</sub>-UO<sub>2</sub> pellets were treated with Sulfex decladding solution in air, the uranium loss for a 3-hr contact was twice that when air was excluded; the loss rate in air after 3 hr was 0.01% per hour. In the absence of air, no increase in loss resulted when the dissolution was done in a 1-w/liter Co<sup>60</sup> gamma-ray field.

Welded specimens of vacuum-induction-melted, low-carbon Ni-o-nel appeared to be free of localized attack in the heat-affected zone after 96 hr exposure to Thorex dissolver solutions. Preferential edge attack of Haynes experimental alloys EB4358 and EB5459 in boiling Sulfex solution was eliminated by smoothing the cut edges of the specimens; however, random pitting was not eliminated.

Fluoride Volatility Processing. - Adaptation of the fused-salt volatility method for processing stainless-steel-containing fuel appears feasible, but the optimum flowsheet will be a compromise with respect to dissolution and corrosion rates, structural metal fluoride solubility, and whether uranium is recoverable by fluorination.

"Flinak" (42.0 mole % KF, 46.5 mole % LiF, 11.5 mole % NaF) gives the highest dissolution rate and metal capacity of any melt tested. The rates were 9.7, 8.5, and 5.5 mg cm<sup>-2</sup> min<sup>-1</sup>, respectively, at 550, 600, and 650°C. The solubility of type 347 stainless steel is approximately 3% based on analyses of filtered salt samples. The corrosion rate at 600°C is 0.33 mg cm<sup>-2</sup> min<sup>-1</sup> for "A" nickel and 0.0011 mg cm<sup>-2</sup> min<sup>-1</sup> for copper. Uranium volatilization is not feasible unless 25 to 50 mole % ZrF<sub>4</sub> is added to the "flinak."

Other melts are being tested to permit processing of the melted-down EBR core 2 in the existing INOR-8 dissolver in the volatility pilot plant.

A temperature-zoned movable-bed sorption unit containing NaF pellets demonstrated reliable discharge of HF-saturated and caked NaF pellets with a maximum hydraulic cylinder pressure of 140 psig.

Eleven tests were made on the dissolving of 2 x 2 in., ten-plate Zircaloy-2 coupons in an HF-sparged melt consisting of 43 mole % NaF and 57 mole % LiF together with 0 to 45 mole % ZrF<sub>4</sub>, at temperatures of 525 to 700°C. The maximum "instantaneous" dissolution rate was 12 mg cm<sup>-2</sup> min<sup>-1</sup> at 700°C and zero ZrF<sub>4</sub> concentration. The average rates ranged from 0.8 to 4 mg cm<sup>-2</sup> min<sup>-1</sup>. These data showed a small temperature effect and a larger effect due to ZrF<sub>4</sub> concentration changes. The magnitude of these effects seems to depend on the absolute concentration of ZrF<sub>4</sub>.

## PHYSICAL RESEARCH PROGRAM

Reactor Operations. - Installation of equipment for annealing the Graphite Reactor is being continued and is expected to be completed early in August. It is now planned to conduct the annealing during the Labor Day weekend.

Installation of the 30-Mw cooling system at the ORR is in progress and is proceeding on schedule. The 5-1/2-ft-dia shielding plug in the south engineering testing facility was removed and replaced successfully. By removing fuel, shielding inside the lattice, and removing all but one experiment, it was possible to reduce radiation in the mouth of the open hole to less than 10 mr/hr.

Waste Disposal. - The new intermediate-level waste disposal trench is now in operation and is seeping waste at the rate of about 4500 gal/day. This trench is covered, so that no radiation reaches ground level, and no seepage through the soil has been detected around the trench. Work has started toward covering open pit No. 4; eventually this will be completely filled with shale and stone and covered with a waterproof seal to prevent surface water from entering. Both the new trench and pit No. 4 have been treated with copper to help fix the ruthenium in liquid waste.

Monitoring results for approximately six weeks have been obtained from grab samples from White Oak Creek and tributaries. These have indicated an increasing amount of strontium in Melton Branch. Practically no strontium was found in the tributaries from the pit area.

## PHYSICS AND MATHEMATICS RESEARCH

Charge Spectrometry. - The charge and recoil spectra of the ions formed following  $\text{He}^6 \xrightarrow{\beta^-} \text{Li}^6$  were measured and compared with theoretical expectations. Because of the availability of appropriate wave functions describing the ground state of helium and several states of Li II, Winther [Kgl. Danske Videnskab. Selskab, Mat.-fys. Medd. 27, No. 14 (1953)] has been able to calculate the electron shake-off following  $\beta^-$  decay more rigorously than is generally possible. He predicts the loss of one electron in  $(10.5 \pm 1.5)\%$  of the decays; here, it was found to be in  $(10.6 \pm 1.0)\%$ . He further states that the chance for the loss of two electrons is less than 1 part in 1000. This is consistent with the finding here of  $(0.04 \pm 0.01)\%$  for charge 3.

Winther also suggested that the recoil energy could account for a shake-off of an electron in about 0.3% of the  $\text{He}^6$  decays for the most energetic ion. It should be noted that this energy ( $\sim 1500$  ev) is exceptionally large for  $\beta^-$  decay. Comparison of the recoil energy spectra of  $\text{Li}^+$  and  $\text{Li}^{++}$  leads to an experimental figure of  $(0.7 \pm 0.5)\%$ .

Comparison of the relative intensities of  $\text{Li}^{+++}$  at two different recoil energies, furthermore, shows a strong dependence for the triply charged ion on recoil energy. About two-thirds of the charge-3 ions formed from  $\text{He}^6$  would seem to require kinetic energy for their formation.

Neutron Diffraction. - Magnetic and thermal measurements at Ames on polycrystalline holmium exhibit anomalies at about 132°K and near 20.0°K which are indicative of magnetic ordering transitions. Single-crystal and powder neutron diffraction data which have now been obtained show the higher temperature anomaly to be a transition from the paramagnetic state to an ordered magnetic structure of the helical type. In this structure the screw axis is the c axis of the crystal, and the moments are parallel in, and parallel to, the (00H<sub>3</sub>) planes. The interplanar turn angle decreases linearly with decreasing temperature from 48.8° at 119°K to 38.4° at 52°K. For temperatures above about 35°K the map of scattering density in reciprocal space shows only a single pair of satellites disposed symmetrically, along the b<sub>3</sub> axis, about the normal reciprocal lattice points. In particular, a very intense pair of magnetic reflections is observed at very small angles corresponding to satellites associated with the origin (0,0,0). A careful search in the vicinity of the origin revealed no secondary satellites: the sensitivity of the search was such that a secondary satellite 0.01% as intense as the primary one would have been detected.

Theoretical Physics. - A one-body spin-orbit potential for spin-1 particles may contain, in addition to the familiar vector term  $\underline{l} \cdot \underline{s}$  used with spin-1/2 particles, certain tensor terms T. The T may be constructed from the position, momentum, and angular momentum vectors of the particle. Time reversal invariance cannot be demanded if a complex potential is allowed, but the requirements of parity conservation and symmetry of the scattering matrix allow only three forms of T. Only one of these remains diagonal in the orbital angular momentum. A simple model may be used to illustrate the possible origin of a tensor coupling for deuterons.

Inelastic scattering is closely analogous to an electric multipole radiative transition and will show similar collective enhancement. Spin-flip transitions are little affected, the enhancement being found in the non-spin-flip amplitudes. Such enhancement will modify the conclusions drawn about angular momentum coupling in the target nucleus, especially in the p shell, since these depend upon the ratio of spin-flip to non-flip.

High-Voltage Experimental Program. - Millimicrosecond time-of-flight techniques, used for studying total cross sections of separated isotopes from 3 to 50 keV for nuclei A = 45 to 88, have resulted in the determination of s-wave level densities and strength functions. Average radiative capture cross sections for A = 79 to 197 and energies 7 to 170 keV provided p-wave strength functions and estimates of s-wave level densities.

The role of phase shifts of neutron scattering used in combination with bound-state information in defining phenomenological nuclear potentials has been illustrated for the case of O<sup>16</sup>. Various forms of the potential have been compared. Data on the total neutron cross section of Pb<sup>208</sup> from 0.55 to 4.32 MeV show up a great many new resonances.

Spectroscopy Research Laboratory. - The infrared spectra of solid phosphine and the deuterated phosphines have been observed at temperatures between 112 and 4°K. Samples were prepared by the slow deposition of solid upon the surface of a cooled CsBr disk. Two spectra were observed, corresponding to two solid phases with a transition in the region 85 to 90°K.

There was no indication of the phase transition near 30°K reported by Clusius from heat capacity measurements. The spectra recorded from the low-temperature solid phase, below 85°K, can be interpreted on the basis of a molecular crystal of low symmetry and weak intermolecular coupling. The higher temperature phase, above 90°K, provides spectra which indicate a crystal of high symmetry, but which cannot be satisfactorily interpreted on the basis of weak coupling in the molecular lattice.

## CHEMISTRY RESEARCH

Spectrophotometric Studies of Solutions at Elevated Temperatures and Pressures. - Spectrophotometric study of aqueous solution chemistry at temperatures up to 330°C and pressures up to 200 atm was started. A spectrophotometer capable of operating under these extreme conditions is being designed and built. The instrument, after necessary development, may provide an in-line analytical system for fluid fuel reactors for high-temperature-pressure processes and will serve for basic chemical research.

With static solutions in thermostatted cells, spectral studies have been made at atmospheric pressure on sulfate and perchlorate systems of uranium, copper, and nickel as a function of temperature and other solution variables up to 100°C. A mathematical technique utilizing high-speed digital computation was developed to resolve the seriously overlapping spectral bands and fine structure. Spectra of uranyl perchlorate and uranyl sulfate were completely resolved into the individual components. These techniques allow a quantitative study to be made of complex ion formation, etc., in solution as a function of temperature and other parameters. Results of this work to date, especially on the uranium spectra, showed that the least-squares non-linear iterative matrix programs that have been modified for this use are entirely adequate for the analysis of such systems. It has been demonstrated that the computer programs can handle overlapping electronic and vibrational bands, and also electronic bands with vibrational fine structure. Correlation of these phenomena with complex ion formation is in progress.

Raw Materials Research and Development. - Since granitic rock represents the most extensive future low-grade source of thorium, evaluation studies are being made of processing methods and costs for recovering thorium from this material. Thus far, 12 granite samples have been obtained which range from 10 to 95 ppm in thorium concentration. In sulfuric acid leaching tests, thorium recoveries varied between 25 and 80%, and consumption of sulfuric acid was high, ranging from 40 to 120 lb per ton of granite. The differences in recoveries were apparently due to variation in mineralization. Filtration of the leached pulp, otherwise extremely slow, was rapid after treatment with Separan 2610.

Solvent Extraction Research. - Radiation-induced chemical nitration products of Amsco 125-82 were more detrimental to solvent cleanup in tributyl phosphate extraction processes than the accompanying degradation of the tributyl phosphate. Tributyl phosphate containing HNO<sub>3</sub> in a 4:1 mole ratio was irradiated by a Co<sup>60</sup> gamma-ray source and then diluted to 1 M with unirradiated Amsco 125-82 (solution 1). A similar solution was irradiated as a 1 M solution in Amsco 125-82 (solution 2). Both solutions were

scrubbed with dilute aqueous sodium carbonate to remove low-molecular-weight acids. The Zr-Nb extraction coefficient for solution 1 decreased slightly with irradiation up to 45 whr/liter; that for solution 2 increased by a factor greater than 10 and was decreased to its original value only by extensive treatment with a solid sorbent.

The tertiary amine extraction process for separating technetium, neptunium, and uranium from fluorination plant residues (ORNL-2874) was tested in a continuous countercurrent experiment. The recoveries from an actual plant solution, expressed as percentages of the amount in the feed and adjusted for material balance, were as follows:

	Tc	Np	U
Uranium product	2	6	100
Neptunium product	0.1	94	0.05
Technetium product	98	<0.1	<0.001
Raffinate	<0.2	<0.1	0.003

The material balances were 103 to 107%. Thorium was split 60% with uranium and 40% with neptunium, and was the chief contaminant in the neptunium product. A trace of protactinium, the most radioactive contaminant in the feed, went chiefly with the neptunium.

Uranium extraction isotherms obtained with trilaurylamine from acid aluminum nitrate process solutions (fluorination plant residue leach solution) did not conform to the usual extraction coefficient relation

$$E = E_1 \underline{M} (\underline{M} \text{ amine} - n \underline{M} \text{ U})^x$$

with any one value of  $n$ , but indicated that  $n$  increases as the ratio of extracted uranium to total amine decreases. To separate the effects of  $n$  and  $x$ , uranyl nitrate was extracted from 1  $\underline{M}$   $\text{HNO}_3$ -1.66  $\underline{M}$   $\text{Al}(\text{NO}_3)_3$  solution with 0.1, 0.3, and 0.5  $\underline{M}$  trilaurylamine. The resulting extraction isotherms showed that  $x = 1$  at low uranium loading ratios, and  $x \approx 1$  at equal loading ratios up to U/amine ratios of at least 1/5. These extraction isotherms, like those from process solutions, indicated that  $n$  varies with uranium loading, the number of moles of amine per mole of uranium being 2.5 or less at saturation and 4 or more when the ratio of extracted uranium to total amine is 1/10 or less.

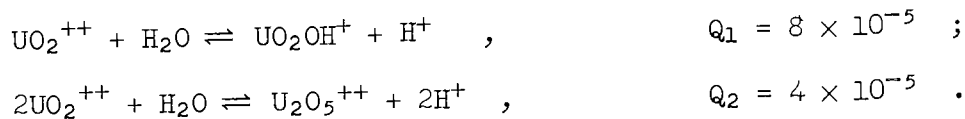
Ion Exchange Technology. - The self-diffusion of uranyl sulfate in Dowex 21K resin was studied with a submerged pump contactor at various solution flow rates. At a high flow rate, 10 ml  $\text{sec}^{-1} \text{cm}^{-2}$ , particle diffusion appeared to be the rate-controlling step. The self-diffusion coefficients were  $4.4 \times 10^{-8}$  and  $2.60 \times 10^{-8} \text{ cm}^2 \text{ sec}^{-1}$  for resin beads of 1200 and 960  $\mu$  respectively. Samples containing 20 to 25 beads per sample were required in order to decrease the data scatter to an acceptable level.

Mechanisms of Separations Processes. - Radiation damage to tributyl phosphate (TBP) leads to the formation of dibutylphosphoric acid, monobutylphosphoric acid, and orthophosphoric acid, whose determination in solutions

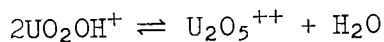
containing Amsco 125-82, nitric acid, and water have proved very difficult. A method that appears promising involves separating the acids from each other and from other solution components by ascending paper chromatography, cutting the paper into short sections, irradiating these sections in a neutron flux of  $\sim 10^{13}$  neutrons  $\text{cm}^{-2} \text{sec}^{-1}$  for 1 hr, and finally counting the beta rays of the  $\text{P}^{32}$  formed by the neutron activation. Accuracies are of the order of  $\pm 20\%$  when the phosphorus content of an individual phosphoric acid is as low as 0.02 g per liter of solution.

The solubilities of ferric monobutylphosphate (MBP) and ferric dibutylphosphate (DBP) in aqueous nitric acid and in 30% TBP-Amsco- $\text{HNO}_3$  solutions were determined. The solubility of  $\text{Fe}_2(\text{MBP})_3$  in the aqueous phase increased from  $1.8 \times 10^{-4}$  to  $8 \times 10^{-2}$  M, and the solubility in the organic phase increased from less than  $1.4 \times 10^{-4}$  to  $3.4 \times 10^{-2}$  M as the concentration of nitric acid in the aqueous phase was increased from 0 to 2.96 M, corresponding to 0 to 0.64 M  $\text{HNO}_3$  in the organic phase. The solubility of  $\text{Fe}(\text{DBP})_3$  was below the spectrographic limit of detectability,  $\sim 1 \times 10^{-5}$  M, in the organic phase and increased from less than  $1 \times 10^{-5}$  to  $\sim 4 \times 10^{-4}$  M as the acidity in the aqueous phase was increased from 0 to 3.2 M.

High-Temperature Aqueous Solution Chemistry. - Further measurements of uranium hydrolysis at  $94^\circ\text{C}$  were made with the glass electrode concentration cell previously described (ORNL-2874). In these tests total uranium concentrations in the range from 0.002 to 0.01 M and equilibrium acid concentrations in the range from 0.0005 to 0.02 M were studied in 0.5 M nitrate solutions. The results are consistent with the following hydrolysis equilibria and equilibrium quotients:



The values of  $Q_1$  and  $Q_2$  at  $25^\circ\text{C}$  (reported in the literature) are about  $8 \times 10^{-7}$  and  $1 \times 10^{-6}$  respectively. Thus these quotients increase rapidly with temperature. The dimerization equilibrium



is also very temperature dependent, its quotient  $Q_d = Q_2/Q_1^2$ , however, decreasing with temperature from  $2 \times 10^6$  at  $25^\circ\text{C}$  to  $6 \times 10^3$  at  $94^\circ\text{C}$ . The approximate heats of reaction from these values of  $Q_1$ ,  $Q_2$ , and  $Q_d$  at the two temperatures are 15, 12, and -18 kcal respectively.

Reactor Neutron Cross Sections. - An upper limit of about  $7 \times 10^5$  years was arrived at for the half life of  $\text{Bi}^{208}$ . This result was obtained by measuring the disintegration rate and measuring qualitatively the  $\text{Bi}^{208}/\text{Bi}^{209}$  mass ratio for a sample of  $\text{Bi}^{208}$  which had been made by an (n,2n) reaction on bismuth during a reactor irradiation and which had been further concentrated with respect to  $\text{Bi}^{209}$  by an electromagnetic separation. The conclusion concerning the half life is consistent with an approximate estimate of  $7.5 \times 10^5$  years by C. H. Miller and co-workers at Chalk River.

A value of 870 barns was determined for the fission resonance integral of  $\text{U}^{233}$  from analyses of three fission products:  $\text{Sr}^{89}$ ,  $\text{Mo}^{99}$ , and  $\text{Ba}^{140}$ .

This value may be compared with two values, 900 and 820 barns, calculated from resonance data in BNL-325.

Nuclear Chemistry: Characterization of Short-Lived Fission Products. -

A preliminary energy spectrum of the delayed neutrons from 4.1-sec  $N^{17}$  was determined. The source was prepared by neutron irradiation of  $Li_3N$ , enriched in the isotopes  $Li^6$  and  $N^{15}$ . Tritons from the reaction  $Li^6(n,\alpha)T$  formed the desired activity by the reaction  $N^{15}(t,p)N^{17}$ . Neutron energy measurements were performed by a time-of-flight technique, the emission of a beta particle being used to establish the time at which the neutron was emitted. Experiments performed with flight paths of 50 and 75 cm and an energy resolution of about 20% gave identical neutron results within the experimental error. An average of four determinations yielded an energy of  $1.08 \pm 0.05$  Mev for the most energetic neutron group. After the kinetic energy is corrected for nuclear recoil, the transition energy to the ground state of  $O^{16} + n$  is  $1.15 \pm 0.05$  Mev.

Electrochemical Kinetics and Its Application to Corrosion. - The behavior of benzoate ion as an inhibitor for the dissolution of iron in acid media was investigated by cathodic polarization. Addition of the inhibitor to an acid perchlorate solution at fixed pH leaves the corrosion characteristics of the electrode essentially unchanged until the formal concentration of the inhibitor reaches a value of about  $1 \times 10^{-3}$ . Between  $1 \times 10^{-3}$  and  $1 \times 10^{-1}$  f the inhibitor is adsorbed, with an ennobling of the open-circuit potential and a great decrease in the corrosion rate. At a fixed concentration of inhibitor, the corrosion potential becomes less noble by about 60 mv for each unit by which the pH is raised. Also, at a fixed concentration of inhibitor, the corrosion rate is independent of pH, at least up to a pH of 5.3, again as in the absence of inhibitor. The data show that adsorption of the inhibitor increases the overvoltage of both the anodic and the cathodic processes, the larger effect being on the anodic process.

Potentiostatic and galvanostatic measurements, together with spectrophotometric studies on important association equilibria, provided considerable insight into the mechanism whereby thiocyanate ion catalyzes the overall reduction rate of cupric species on passive stainless steel in oxygenated acid sulfate solutions.

Interpretation of electrochemical kinetic data on systems containing cupric, sulfate, and thiocyanate ions may be greatly facilitated by an understanding of the complexing effects in these systems. Values of the 1:1 association quotients of  $Cu^{++}$  with  $SO_4^{--}$  and of  $Cu^{++}$  with  $SCN^-$  were measured spectrophotometrically as a function of temperature from 25 to 65°C in sodium perchlorate-perchloric acid solutions of selected ionic strengths. The (concentration) association quotient  $K_c$  of  $Cu^{++}$  with  $SCN^-$  is given as a function of the absolute temperature T by the following equations:

$$\text{for an ionic strength of } 0.05 \quad , \quad \log K_c = -0.283 + \frac{6.79 \times 10^2}{T} \quad ;$$

$$\text{for an ionic strength of } 0.50 \quad , \quad \log K_c = -0.391 + \frac{6.44 \times 10^2}{T} \quad .$$

The 1:1 association quotient of  $\text{Cu}^{++}$  with  $\text{SO}_4^{--}$  is given as a function of temperature at an ionic strength of 0.30 by the equation

$$\log K_c = 2.01 - \frac{3.26 \times 10^2}{T}$$

In a continued study of cathodic processes related to corrosion, further research was carried out on the reduction of oxygen on zirconium and certain of its alloys. The effect of change of pH was determined, and the conditions under which the kinetic order of reduction changes from unity to fractional orders were clarified. The studies are being extended to a Zr-15 wt % Nb alloy. As compared with the results for crystal-bar zirconium, the data obtained so far show that the kinetic parameters of the cathodic process are unchanged but that the parameters of the anodic process are significantly different. This may indicate that the metal ion, rather than the oxide ion, is involved in the rate-determining anodic process.

Chemical Separation of Isotopes. - The isotopic fractionation factors for both oxygen and carbon were measured at several temperatures between  $\text{CO}_2$  gas and liquid dipropylamine carbamate. The results are presented below:

Temperature (°C)	$\frac{(C^{12}/C^{13})_{\text{gas}}}{(C^{12}/C^{13})_{\text{liq}}}$	$\frac{(O^{16}/O^{18})_{\text{liq}}}{(O^{16}/O^{18})_{\text{gas}}}$
25	1.0059	1.0081
38	1.0046	1.0090
60	1.0028	1.0096

Chemical Applications of Nuclear Explosions. - In studies on the chemistry of contained nuclear explosions, tritium exchange from water vapor to molecular hydrogen flowing over solid calcium sulfate at 380°C was 0.07% per gram of  $\text{CaSO}_4$  initially and 2.7% per gram after 40 min with a hydrogen-to-water-vapor flow ratio of 20.

Under static conditions the rate of reduction of calcium sulfate by hydrogen at 700°C was virtually independent of hydrogen pressure between 200 and 500 mm Hg when the  $\text{CaSO}_4$  surface area was constant. The mechanism of the reaction is not known at present. The rates of reduction of calcium sulfate at constant volume were 0.14 and 0.12  $\text{mm m}^{-2} \text{min}^{-1}$  for calcium sulfate powders with surface areas of 2.9 and 0.82  $\text{m}^2/\text{g}$  respectively. Calcium sulfate is readily decomposed to calcium oxide when fine powders of  $\text{CaSO}_4 \cdot 1/2\text{H}_2\text{O}$  are sprayed into a plasma jet.

Thermal decomposition of ammonium bicarbonate was too slow to allow its use as a filter in the Gnome sample pipe, ~ 20 min being required for decomposition of 10 g of the powdered material at temperatures of 100 to 200°C.

## METALLURGY AND MATERIALS RESEARCH

Ceramics Research. - Thoria powder pressed at 15,300 psi forms pellets with densities in the range from 4.2 to 6.4 g/cc, depending on the status of the powder. Calcination at 1200°C gave densities of 5.10 to 8.08, whereas calcination at 1800°C resulted in densities of 6.73 to 9.86. Thoria consisting of vitreous chunks from hydroxide precipitation or previously high-fired thoria tended to give pellets with the highest green density and to undergo the least sintering. Sintering of thoria batches prepared by oxalate precipitation with different lengths of digestion in the supernatant liquid demonstrated that sintering of more compact or solid particles (those obtained by long digestion) proceeds less readily than sintering of more porous particles. It has not yet been possible to correlate porosity and sintering with grain size in the various thoria preparations because of difficulty in observing the grain size.

Preliminary studies on the microstructure of fused  $UO_{2+x}$  ( $x = 0.05, 0.09,$  and  $0.14$ ) have shown that the distribution of the  $U_4O_9$  phase in the  $UO_2$  matrix is dependent upon the body composition and on the rate of cooling from the single-phase region. By quenching in oil or in water from 1000°C, a supersaturated single phase, free of  $U_4O_9$ , can be obtained with O/U ratios up to 2.09. Cooling in air results in a dispersion of  $U_4O_9$  in the  $UO_2$  which is finer than that obtained on cooling in the furnace. These results substantiate the accepted phase relations between  $UO_2$  and  $U_4O_9$  and suggest that lattice parameter shifts of the single-phase products can be used for determining O/U ratios.

Efforts to grow stoichiometric  $UO_2$  crystals from fluoride melts by utilizing argon as a water carrier are continuing. The resulting melts are processed in ammonium oxalate to remove unreacted fluorides. Thermogram, DTA, x-ray, and petrographic analyses have shown that stoichiometric  $UO_2$  has been produced.

## CONTROLLED THERMONUCLEAR RESEARCH

Cross-Section Studies. - An ORNL-made silicon barrier detector has been calibrated by measuring the energies of neutral particles in the DCX. The detector is linear in its energy response to  $H^0$  and  $H_2^0$  particles and has a resolution of 11% for 300-keV  $H^0$ . The response of the detector is not influenced by operation in a strong (10-kilogauss) magnetic field. The detector will be used to measure neutral-particle energy distributions in the DCX.

DCX-1 Facility. - Operation with the three-electrode (i.e., cathode, anode, and reflector) deuterium arc has revealed that the arc diameter increases with either an increase in arc current or a decrease in deuterium gas input. For arc currents of approximately 100 amp and gas flows of 3 to 4 atm cc sec<sup>-1</sup>, the arc diameter is 1-3/4 in. at the anode position, which is the center of the anode extension coil. By way of comparison, at the cathode position, which is near the center of the other extension coil, the arc seems to be confined to the tip of the 3/4-in.-dia electrode.

Initial experience with a rotating water-cooled anode indicates that it will be possible to operate this type of two-electrode gas arc without

significant anode deterioration at gas flows lower than the 4 to 5 atm. cc sec<sup>-1</sup> previously required.

Data for a mass spectrometer analysis of the residual gas components in the vacuum system have been taken. With an H<sub>2</sub><sup>+</sup> beam entering the DCX the major gas component in the vacuum system is H<sub>2</sub>. Other components of significance are N<sub>2</sub>, CO, H<sub>2</sub>O, O<sub>2</sub>, and various hydrocarbon fractions.

DCX-EPA. - Some preliminary data have been obtained on the operation of a gas arc with a hollow tungsten cathode and a rotating water-cooled anode. The arc is characterized by a very large transport of charged particles across the magnetic field. Typical conditions for a nitrogen arc are: arc voltage 1000 v, arc current 150 amp, and gas feed 1 cc/sec. Satisfactory operation with the reflux arc has also been achieved. These experiments have been made possible by changes in the mounting system of the electrodes and shields.

DCX-EPA is in the process of being moved to Building 9201-2 and will be inactive for at least two months.

Ion Source Development. - An analyzing system for high-current ion beams at 60 to 100 kv has been installed and tested. The einzeln lens used, which is the result of an attempt to obtain the greatest possible current in a parallel beam with 2 to 3 in. diameter, limits the maximum hydrogen current that can be analyzed to approximately 100 ma. Numerous changes have been made in the Von Ardenne-type ion source in an effort to maximize the H<sub>2</sub><sup>+</sup> beam fraction. Under optimum operating conditions, the H<sub>2</sub><sup>+</sup> beam component is 70 to 80% in the current range from 20 to 50 ma and 60 to 70% with a beam current of 50 to 100 ma. Extracted currents greater than 100 ma per ampere of arc current have been obtained with a source geometry which, unfortunately, yields lower H<sub>2</sub><sup>+</sup> fractions.

The 600-kv beam test facility has been installed, and preliminary high-voltage tests have been carried out on the insulator supports and the accelerator tube. Despite numerous sparks, with voltages up to 475 kv, no significant damage to the tube has been observed. Further tests are currently in progress.

Theory. - The general program for derivation of the coefficients of the Fokker-Planck equation from several principles continues. Exact relativistic solutions have been obtained for the case of an infinite, uniform field-free plasma. A similar technique appears to be applicable in the more interesting case of a uniform magnetic field, and this result should be completed shortly.

A study of possible effects of a plasma potential on the DCX steady state is continuing.

## BIOLOGY AND MEDICINE PROGRAM

### RADIATION EFFECTS ON BIOLOGICAL SYSTEMS

Cell Growth and Reproduction. - Ten minutes exposure of the protozoan Tetrahymena to nutrient medium containing tritiated cytidine results in labeling of the ribonucleic acid of the nucleus only. When cells so labeled

are transferred to a nonradioactive medium, the radioactivity of the nucleus shifts to the cytoplasm over a period of 1 to 2 hr. The results are considered to constitute strong evidence for the continuous transfer of ribonucleic acid from the nucleus to the cytoplasm.

Pathology and Physiology. - Mice of the (C57L × A/H<sub>e</sub>)F<sub>1</sub> and RF strains subjected early in life to acute whole-body ionizing radiation died prematurely with certain neoplasms and other pathologic changes that occurred late in life among nonirradiated controls. Some of these changes (e.g., thymic lymphoma, granulocytic leukemia, Harderian gland tumor, ovarian tumor, pituitary tumor, cataract of lens, atrophy of iris, nephrosclerosis) were increased in incidence and severity, and others (e.g., lung tumor, mammary sarcoma, nonthymic lymphoma, subcapsular ovarian cyst) decreased; thus the irradiated populations were not identical with the controls in all respects other than premature mortality. Nevertheless, at any given radiation dose level, most changes were hastened in onset to a similar degree, suggesting alteration of a common "biological clock" mechanism, or advancement of the aging process.

Biophysics: Magnetic Resonances. - Previously reported preliminary electron spin resonance measurements on irradiated dry lettuce seeds and experiments on the protection of the same material with S,2-aminoethylisothiourea (AET) have been extended. The results indicate that (1) about 300 ev is dissipated per free radical produced by very low doses of 300-kv-peak x rays; (2) there is a saturation limit of almost  $10^{18}$  radicals per gram; (3) the decay of radical concentrations  $N(t)$  with time  $t$  is empirically best described by the formula

$$N(t) = N(1) - \alpha \ln t ,$$

for which no suitable statistical model has been found; (4) almost 90% of the observed radicals are produced in the embryo; (5) the decay rates are increased by increases in moisture or temperature; (6) the inhibition of germination resulting from exposure to 500 kr is partly reversed by preirradiation AET treatments which do not reverse the inhibition of germination by a "radiomimetic" chemical (maleic hydrazide); and (7) the concentration of free radicals immediately after irradiation is higher and their decay more rapid for the AET-treated seeds than for controls.

Biophysics: Ultraviolet Studies. - Spores of Streptomyces griseus show excellent photoreactivation, as is well known. Under similar conditions, however, it has been found that they fail to show significant photoprotection. It is now clear that photoprotection is considerably less universal than photoreactivation.

Further investigation of the synergistic action of x rays and ultraviolet radiation on chromosome breakage in dry pollen has shown this phenomenon to be much more sensitive than was first realized. The effect is clearly demonstrable with as little as 0.25 r of 250-kv-peak x rays in combination with  $0.01 \times 10^6$  ergs/cm<sup>2</sup> of 2650-A ultraviolet radiation. Further studies of the variation of the effect with the time intervals between the treatments are in progress.

Techniques for irradiating growing pollen tube cultures have been perfected. Photoreactivation of ultraviolet damage to dry pollen has been demonstrated when the photoreactivating light is delivered to the growing cultures.

Chemical Protection and Enzyme Catalysis. - An improved procedure has been devised for the purification of mitochondrial malic dehydrogenase in which several unwieldy steps are eliminated. Chromatography of the enzyme on diethylaminoethyl cellulose has been incorporated into the isolation procedure, replacing multiple starch zone electrophoresis runs. This improvement has facilitated the separation of highly active enzyme in larger quantities than previously, as well as permitted the isolation of a purified, active supernatant malic dehydrogenase.

#### COMBATING RADIATION DETRIMENTAL EFFECTS

Radiation Protection: Living Cells. - Recent evidence presented in the literature suggests that catalase, an enzyme effective in destroying hydrogen peroxide, may be important in determining the sensitivity of yeast cells to ionizing radiation. In an attempt to extend these observations to a group of interrelated bacterial strains, catalase activity, radiation sensitivity, and hydrogen peroxide sensitivity were investigated in these organisms grown under a variety of conditions. The conclusions are that, for the organisms under consideration, total catalase activity is not related to sensitivity to either radiation or hydrogen peroxide. There is, however, a good correlation between radiation sensitivity and hydrogen peroxide sensitivity in this group of organisms. This suggests that hydrogen peroxide production may well be one means by which ionizing radiation inactivates cells, and that if catalase is important at all, its intracellular distribution must be taken into account.

Mammalian Radiation Recovery. - Progress has been made on the problem of whether irradiated mice treated with bone marrow develop antibody-forming cells of donor or host type. Recent studies showed that mice irradiated and treated with fetal or adult foreign bone marrow have functioning antibody-forming cells of the donor marrow type.

Histological surveys on normal mice injected either once or twice with foreign bone marrow confirmed the previous finding that a special group of cells in lymphatic tissues, known as the germinal center cells, are the first to respond to an antigenic material.

Biochemical studies on the liver of irradiated mice treated with foreign bone marrow and undergoing the immunologic disorder known as secondary disease demonstrated marked biochemical changes in the liver. A marked increase in liver weight was also observed.

Radiation Immunology. - In confirmation of previous studies demonstrating agglutinin (anti red blood cell) production by spleen cells in diffusion chambers of 0.1  $\mu$  porosity, it has been possible to detect immunohistochemically the production of precipitin (anti bovine serum albumin) by spleen cells of primed rabbits. The diffusion chambers were implanted into

homologous nonirradiated rabbits and x-rayed (600 r) mice. Viable, antibody-synthesizing lymphoidal and plasmocytic cells were detected after up to 12 days when x-rayed mice were used as recipients. In contrast, most of the cells detected seven days after culturing in homologous rabbits were large, mononuclear, non-antibody-containing cells.

Under the optimum condition for the PCA (passive cutaneous anaphylaxis) test it was found that the sensitivity of the reaction is dependent on the genetic relation between the test animal and the source of antibodies; in the mouse, the order is antibodies of mouse > rat > guinea pig > rabbit > chicken.

With the recently devised model for assay of homologous hematopoietic transplantation antigens, it was found that the RD<sub>50</sub> dose (the priming dose of donor antigen capable of stimulating the host to reject 50% of the donor spleen cells) is 100 for viable bone marrow cells and 10,000 for dead bone marrow, liver, and testicular cells.

#### BIOMEDICAL PROBLEMS IN ATOMIC ENERGY OPERATIONS

Basic Instrumentation. - The development of a fountain-pen-sized personal radiation monitoring instrument has been completed. Immediate alarm indications that are proportional to the dose rate of gamma or hard beta radiation are given by a flashing neon lamp and by an audible screamer. The flashing rate of the lamp and the pitch of the screamer are proportional to radiation intensity over a dynamic range extending from background to about 1 r/hr. Above this level the alarms continue at their maximum indication up to at least  $3 \times 10^6$  r/hr without blocking. Continuous operation for over a month is obtained from a 4-v mercury battery. A miniature Geiger counter detector is used in a circuit having three transistors and five semiconductor diodes. A quantity of these instruments is being procured for use by the Laboratory.

OPEN LITERATURE PUBLICATIONS

- Adams, R. E., W. E. Berry, J. A. Milko, S. H. Paine, R. S. Peoples, and H. A. Pray, "Thorium Alloys," p 227, in Reactor Handbook (ed. by C. R. Tipton, Jr.), 2d ed., vol I, Interscience, New York, 1960.
- Anderson, N. G., and C. B. Norris, "Cell Division. III. The Effects of Amines on the Structure of Isolated Nuclei," *Exptl. Cell Research* 19, 605 (1960).
- Apple, R. F., and J. C. White, "Determination of Thorium Present in Fluoride Salt Mixtures," *Chemist Analyst* 49, 42 (1960).
- Arnold, W. A., and R. K. Clayton, "The First Step in Photosynthesis: Evidence for Its Electronic Nature," *Proc. Natl. Acad. Sci. U.S.* 46, 769 (1960).
- Bender, M. A., T. T. Phan, and L. H. Smith, "Preservation of Viable Bone Marrow Cells by Freezing," *J. Appl. Physiol.* 15, 520 (1960).
- Bollum, F. J., "Oligodeoxynucleotide Primers for Calf Thymus Polymerase," *J. Biol. Chem.* 235(5), PC18 (1960).
- Bridges, W. H., and W. D. Manly, "Cobalt-Base Alloys," p 520, in Reactor Handbook (ed. by C. R. Tipton, Jr.), 2d ed., vol I, Interscience, New York, 1960.
- Brosseau, G. E., Jr., "Genetic Analysis of the Male Fertility Factors on the Y Chromosome of *Drosophila Melanogaster*," *Genetics* 45, 257 (1960).
- Cable, J. W., M. K. Wilkinson, and E. O. Wollan, "Neutron Diffraction Studies of Antiferromagnetism in  $\text{CrF}_2$  and  $\text{CrCl}_2$ ," *Phys. Rev.* 118, 950 (1960).
- Clayton, R. K., "An Intermediate Stage in the  $\text{H}_2\text{O}_2$ -Induced Synthesis of Catalase in *Rhodopseudomonas spheroides*," *J. Cellular Comp. Physiol.* 55, 9 (1960).
- Clayton, R. K., "Kinetics of  $\text{H}_2\text{O}_2$  Destruction in *Rhodopseudomonas spheroides*: Roles of Catalase and Other Enzymes," *Biochim. et Biophys. Acta* 40, 165 (1960).
- Clayton, R. K., "Physiology of Induced Catalase Synthesis in *Rhodopseudomonas spheroides*," *J. Cellular Comp. Physiol.* 55, 1 (1960).
- Cohn, W. E., "Pseudouridine, a Carbon-Carbon Linked Ribonucleoside in Ribonucleic Acids: Isolation, Structure, and Chemical Characteristics," *J. Biol. Chem.* 235, 1488 (1960).
- Congdon, C. C., and A. Hollaender, "Experimental Applications of Bone Marrow Transplantation," *A.M.A. Arch. Pathol.* 69, 605 (1960).
- Cook, W. H., "Materials for Valves and Bearings in Molten Metals and Fused Salts," p 762, in Reactor Handbook (ed. by C. R. Tipton, Jr.), 2d ed., vol I, Interscience, New York, 1960.
- Darden, E. B., Jr., "Changes in Membrane Potentials, K Content, and Fiber Structure in Irradiated Frog Sartorius Muscle," *Am. J. Physiol.* 198, 709 (1960).

- Dolin, M. I., and N. P. Wood, "The Streptococcus faecalis Oxidases for Reduced Diphosphopyridine Nucleotide. V. Isolation and Properties of a Flavin Mononucleotide-Containing Diaphorase," J. Biol. Chem. 235, 1809 (1960).
- Friedberg, W., "Serum Albumin Metabolism in X-Irradiated Mice with Implanted Rat Bone Marrow," Intern. J. Radiation Biol. 2, 186 (1960).
- Goff, R. A., "The Acute Lethal Response of the Chick Embryo to X Radiation," J. Exptl. Zool. 141, 477 (1959).
- Goodman, C. D., and J. B. Ball, "Survey of (p,d) Reactions at 22 Mev," Phys. Rev. 118, 1062 (1960).
- Greeley, R. S., W. T. Smith, Jr., R. W. Stoughton, and M. H. Lietzke, "Electromotive Force Studies in Aqueous Solutions at Elevated Temperatures. I. The Standard Potential of the Silver-Silver Chloride Electrode," J. Phys. Chem. 64, 652 (1960).
- Haber, A. H., and H. J. Luippold, "Action of 6-(Substituted) Purines on Mitotic Activity in 'Dormant' Lettuce Seeds," Physiol. Plantarum 13, 298 (1960).
- Hamner, R. L., W. D. Manly, and W. H. Bridges, "Carbides and Cermets," p 502, in Reactor Handbook (ed. by C. R. Tipton, Jr.), 2d ed., vol I, Interscience, New York, 1960.
- Harris, L. A., "The Crystal Structure of  $Rb_2ThF_6$ ," Acta Cryst. 13, 502 (1960).
- Holmes, D. K., and G. Leibfried, "Range of Radiation Induced Primary Knock-Ons in the Hard Core Approximation," J. Appl. Phys. 31, 1046 (1960).
- Inouye, H., and W. D. Manly, "Molybdenum and Its Alloys," p 604, in Reactor Handbook (ed. by C. R. Tipton, Jr.), 2d ed., vol I, Interscience, New York, 1960.
- Kenney, F. T., "On the Nature of Adrenocorticoid-Induced Increase in Tyrosine- $\alpha$ -Ketoglutarate Transaminase Activity of Rat Liver," Biochem. Biophys. Research Commun. 2, 333 (1960).
- Kroeger, H., "The Induction of New Puffing Patterns by Transplantation of Salivary Gland Nuclei into Egg Cytoplasm of *Drosophila*," Chromosoma 11, 129 (1960).
- Lynn, W. G., and J. N. Dent, "The Action of Various Goitrogens in Inhibiting Localization of Radioiodine in the Thyroid and Thymus Glands of Larval Tree Toads," Biol. Bull. 118, 430 (1960).
- Makinodan, T., and N. Gengozian, "X-Ray Depression of the Recognition Mechanism of Antibody-Forming Cells," p 339, in Mechanisms of Antibody Formation, Proceedings of a Symposium, Czechoslovak Academy of Sciences, Prague, 1960.
- Makinodan, T., E. H. Perkins, I. C. Shekarchi, and N. Gengozian, "Use of Lethally Irradiated Isologous Mice as in Vivo Tissue Cultures of Antibody-Forming Cells," p 182, in Mechanisms of Antibody Formation, Proceedings of a Symposium, Czechoslovak Academy of Sciences, Prague, 1960.

- Manly, W. D., and W. H. Bridges, "Nickel and Its Alloys," p 636, in Reactor Handbook (ed. by C. R. Tipton, Jr.), 2d ed., vol I, Interscience, New York, 1960.
- Mazur, P., "Physical Factors Implicated in the Death of Microorganisms at Subzero Temperatures," Ann. N.Y. Acad. Sci. 85, 610 (1960).
- McGrath, R. A., "Cell Migration and Abnormal Crypt Cell Enlargement in the Small Intestine of X-Irradiated Mice," Intern. J. Radiation Biol. 2, 177 (1960).
- Moore, F. L., "Liquid-Liquid Extraction of Polonium-208 Tracer from Bismuth Target Solutions," Anal. Chem. 32, 1048 (1960).
- Novelli, G. D., "The Turnover of Pantothenic Acid," p 169, in Fourth International Congress of Biochemistry, vol XI, Vitamin Metabolism (ed. by W. Umbreit and H. Molitor), Pergamon Press, London, 1960.
- Oakberg, E. F., "Irradiation Damage to Animals and Its Effect on Their Reproductive Capacity," J. Dairy Science 43(suppl), 54 (1960).
- Oakberg, E. F., and R. L. DiMinno, "X-Ray Sensitivity of Primary Spermatoocytes of the Mouse," Intern. J. Radiation Biol. 2, 196 (1960).
- Satchler, G. R., "Circularly Polarized Gamma Rays from Direct Nuclear Reactions," Nuclear Phys. 16, 674 (1960).
- Satchler, G. R., and W. Tobocman, "Gamma Rays from Deuteron Stripping Reactions," Phys. Rev. 118, 1566 (1960).
- Slaughter, G. M., W. D. Manly, W. H. Bridges, K. F. Smith, and J. R. Keeler, "Special Purpose Alloys," p 739, in Reactor Handbook (ed. by C. R. Tipton, Jr.), 2d ed., vol I, Interscience, New York, 1960.
- Sonder, E., and L. C. Templeton, "Gamma Irradiation of Silicon. I. Levels in n-Type Material Containing Oxygen," J. Appl. Phys. 31, 1279 (1960).
- Stuy, J. H., "Studies on the Radiation Inactivation of Microorganisms. VI. X-Ray-Induced Breakdown of Deoxyribonucleic Acid in Haemophilus influenzae and in Other Bacteria," J. Bacteriol. 79, 707 (1960).
- Vos, O., J. W. Goodman, and C. C. Congdon, "Donor-Type Lymphatic Tissue Cells in Lethally Irradiated Mice Treated with Homologous Fetal Liver," Transplant. Bull. 7, 408 (1960).
- Watt, W. J., and M. Blander, "The Thermodynamics of the Molten Salt System  $KNO_3$ - $AgNO_3$ - $K_2SO_4$  from Electromotive Force Measurements," J. Phys. Chem., 64, 729 (1960).
- Young, J. P., J. C. White, and R. G. Ball, "Spectrophotometric Determination of Yttrium with Pyrocatechol Violet," Anal. Chem. 32, 928 (1960).

FOREIGN VISITORS

<u>Name</u>	<u>Affiliation</u>	<u>Citizen of</u>
Adam, N. K.	University of Southampton	Great Britain
Bekefi, G.	Massachusetts Institute of Technology	Great Britain
Braun, E. A.	Associated Electrical Industries, England	Israel
Cochrane, C. A.	Tube Investments, Ltd.	United Kingdom
Dalton, G. C. J.	Atomic Energy Commission Research Establishment	Australia
Das, M. S.	Atomic Energy Establishment	India
Dirian, G.	French AEC	France
Duhamel, A. F.	French AEC	France
Ellis, W. R.	AEC, Sydney	Australia
Foelsche, T.	Langley Research Center	Germany
Fredriksson, L. J. G.	Royal Agriculture College	Sweden
Griffiths, D. R.	Atomic Energy Commission Research Establishment	Australia
Gras, M.	French AEC	France
Haaland, A.	Georgia Institute of Technology	Norway
Hagsgard, S. A.	Aktiebologet Atomenergi	Sweden
Hansen, J. A.	Norwegian Health Service	Norway
Hodges, D.	Argonne National Laboratory	Great Britain
Indra, R. N.	Atomic Energy Establishment	India
Kasaka, Y.	University of Michigan	Japan
Larsson, A. H.	Aktiebologet Atomenergi	Sweden
Lawson, J. D.	AERE, Harwell	United Kingdom
McMillan, J. A.	Argonne National Laboratory	Argentina
Mason, R.	Brookhaven National Laboratory	Great Britain
Mazaury, E. C.	French AEC	France
Megaw, W. J.	AERE, Harwell	Great Britain
Morrison, G. C.	Institute for Nuclear Studies	United Kingdom
Murakami, M.	Japan Atomic Energy Research Institute	Japan
Murthy, S. V.	Atomic Energy Establishment	India
Nussbaum, R. N.	Electricite de France	France
Okutsu, H.	Sumitomo Atomic Energy Industries, Ltd.	Japan
Robin, G.	C. E. A., France	France
Rodier, J. F. P.	French AEC	France
Ross, A. H.	A. H. Ross & Associates	Canada
Schonfeld, E.	Radiation Application, Inc.	Argentina
Sheridan, J.	University of Birmingham	Great Britain
Soetangkat, H.	University of Kentucky	Indonesian Republic
Somayaji, K. S.	Atomic Energy Establishment	India
Sommacal, B.	Self	Italy
Sommacal, D.	Self	Switzerland

<u>Name</u>	<u>Affiliation</u>	<u>Citizen of</u>
Turnbull, A. H.	AERE, Harwell	United Kingdom
Venkateswarlu, C.	Atomic Energy Establishment	India
Yokota, R.	Tokyo Shibaura Electric Co.	Japan

Reports issued in this series during the past year:

July 1959	ORNL-2795
August 1959	ORNL-2825
September 1959	ORNL-2845
October 1959	ORNL-2858
November 1959	ORNL-2874
December 1959	ORNL-2895
January 1960	ORNL-2906
February 1960	ORNL-2922
March 1960	ORNL-2932
April 1960	ORNL-2945
May 1960	ORNL-2960
June 1960	ORNL-2980

OAK RIDGE NATIONAL LABORATORY

STATUS AND PROGRESS REPORT

July 1960

Distribution

U.S. Atomic Energy Commission

Oak Ridge Operations Office

1-37. Research and Development Division

External

38. Aeroprojects, Inc.	W. B. Tarpley
39. Allis-Chalmers Manufacturing Co.	W. F. Banks
40-42. Ames Laboratory: Iowa State College	F. H. Spedding
43-45. Argonne National Laboratory	N. S. Hilberry
46. Atomics International (N. Am. Aviation, Inc.)	E. E. Motta
47. Babcock and Wilcox Co. (Atomic Energy Div.)	
48-49. Battelle Memorial Institute	H. W. Russell
50-52. Brookhaven National Laboratory	L. J. Haworth
53. Bureau of Mines, Salt Lake City	J. B. Clemmer
54-61. General Atomic (General Dynamics Corp.)	Manager
62-63. General Nuclear Engineering Corp.	J. West
64-69. Hanford Atomic Products Operation	O. H. Greagor
70-71. Idaho Chemical Processing Plant	R. L. Doan
72. Kaiser Engineers	P. D. Bush
73-74. Knolls Atomic Power Laboratory	K. R. Van Tassell
75-76. Lawrence Radiation Laboratory	H. Fidler
77-78. Los Alamos Scientific Laboratory	N. E. Bradbury
79-80. National Bureau of Standards	L. S. Taylor
81. National Lead Company	C. K. McArthur
82. Nuclear Metals, Inc.	A. R. Kaufmann
83-84. Philadelphia Electric Co.	L. R. Gaty
85. Sanderson and Porter (Atomic Energy Div.)	
86. Union Carbide Corporation	R. W. McNamee
87. Union Carbide Nuclear Company	C. E. Center
88. Union Carbide Nuclear Company	J. L. Gabbard
89. Union Carbide Nuclear Company	D. M. Lang
90. Union Carbide Nuclear Company	J. P. Murray
91-92. USAEC, Chicago Operations Office	
93. USAEC, Lockland Aircraft Reactors Operations Office	H. H. Gorman
94-95. USAEC, New York Operations Office	J. Smith
96-97. USAEC, San Francisco Operations Office	R. Hughey
98-99. USAEC, Savannah River Operations Office	H. Rahner
100. Westinghouse Electric Corp.	A. Squire

Internal

101. K. A. Allen	151. J. C. Griess
102. E. E. Anderson	152. W. R. Grimes
103. C. F. Baes	153. P. A. Haas
104. E. A. Bagley	154. C. S. Harrill
105. P. S. Baker	155. J. C. Hart
106. C. R. Baldock	156. M. R. Hill
107. L. H. Barker	157. C. J. Hochanadel
108. S. E. Beall	158. A. Hollaender
109. E. E. Beauchamp	159. L. B. Holland
110. R. H. Beidel	160. R. W. Horton
111. P. R. Bell	161. F. T. Howard
112. D. S. Billington	162. A. S. Householder
113. C. A. Blake	163. H. H. Hubbell
114. R. E. Blanco	164. G. S. Hurst
115. F. F. Blankenship	165. G. H. Jenks
116. E. P. Blizard	166. R. W. Johnson
117. J. O. Blomeke	167. R. J. Jones
118. A. L. Boch	168. W. H. Jordan
119. E. G. Bohlmann	169. P. R. Kasten
120. C. J. Borkowski	170. G. W. Keilholtz
121. G. E. Boyd	171. C. P. Keim
122. M. A. Bredig	172. G. G. Kelley
123. J. C. Bresee	173. M. T. Kelley
124. R. B. Briggs	174. E. M. King
125. R. E. Brooksbank	175. W. C. Koehler
126. K. B. Brown	176. K. A. Kraus
127. F. R. Bruce	177. Laboratory Shift Supervisor (D. Phillips)
128. W. D. Burch	178. E. Lamb
129. T. H. J. Burnett	179. J. A. Lane
130. A. D. Callihan	180. R. E. Leuze
131. A. E. Cameron	181. W. H. Lewis
132. R. A. Charpie	182. T. A. Lincoln
133. T. E. Cole	183. S. C. Lind
134. C. F. Coleman	184. R. B. Lindauer
135. E. L. Compere	185. R. S. Livingston
136. D. D. Cowen	186. J. T. Long
137. J. A. Cox	187. L. O. Love
138. F. L. Culler	188. R. N. Lyon
139. J. E. Cunningham	189. R. J. Mackin
140. J. S. Drury	190. H. G. MacPherson
141. D. E. Ferguson	191. F. C. Maienschein
142. J. L. Fowler	192. W. D. Manly
143. J. H. Frye	193. M. B. Marshall
144. W. F. Gauster	194. J. A. Martin
145. M. W. Gerrard	195. H. F. McDuffie
146. J. H. Gillette	196. J. R. McNally
147. W. Y. Gissel	197. A. J. Miller
148. H. E. Goeller	198. E. C. Miller
149. C. D. Goodman	199. K. Z. Morgan
150. A. T. Gresky	

- |      |                    |          |   |
|------|--------------------|----------|---|
| 200. | W. L. Morgan       | 226.     | E. G. Struxness   |
| 201. | F. J. Muckenthaler | 227.     | J. C. Suddath   |
| 202. | E. J. Murphy       | 228.     | W. H. Sullivan  |
| 203. | M. L. Nelson       | 229.     | C. D. Susano  |
| 204. | C. E. Normand      | 230.     | J. A. Swartout  |
| 205. | J. L. Need         | 231.     | E. H. Taylor  |
| 206. | G. W. Parker       | 232.     | C. D. Watson  |
| 207. | M. E. Ramsey       | 233.     | B. S. Weaver  |
| 208. | P. M. Reyling      | 234.     | A. M. Weinberg  |
| 209. | A. W. Riikola      | 235.     | M. E. Whatley   |
| 210. | L. P. Riordan      | 236.     | J. C. White   |
| 211. | G. A. Ropp         | 237.     | C. E. Winters   |
| 212. | A. F. Rupp         | 238.     | E. O. Wollan  |
| 213. | A. D. Ryon         | 239.     | R. E. Worsham   |
| 214. | H. C. Savage       | 240.     | W. Zobel  |
| 215. | H. W. Savage       | 241.     | A. Zucker   |
| 216. | A. W. Savolainen   | 242-243. | Central Research Library                                      |
| 217. | H. E. Seagren      | 244.     | Health Physics Library  |
| 218. | E. D. Shipley      | 245.     | ORNL -- Y-12 Technical Library,<br>Document Reference Section |
| 219. | A. Simon           | 246.     | Reactor Experimental Engi-<br>neering Library                 |
| 220. | O. Sisman          | 247.     | Biology Library   |
| 221. | J. R. Sites        | 248-439. | Laboratory Records Department                                 |
| 222. | M. J. Skinner      | 440.     | Laboratory Records, ORNL R.C.                                 |
| 223. | A. H. Snell        |          |   |
| 224. | R. W. Stoughton    |          |   |
| 225. | H. Stringfield     |          |   |